J Comp Physiol A (1985) 157:115–147

Journal of Comparative Physiology A Sensory, Neural, and Behavioral Physiology

Strains in the exoskeleton of spiders

Reinhard Blickhan* and Friedrich G. Barth
Gruppe Sinnesphysiologie, Zoologisches Institut der Johann Wolfgang Goethe-Universität, Siesmayerstrasse 70, D-6000 Frankfurt am Main 1, Federal Republic of Germany

Accepted March 22, 1985

Summary. This is a first attempt to measure strain in the exoskeleton of arthropods during locomotion. The selected sites of measurement at the tibia of large spiders allowed a direct estimation of the mechanical input of slit sense organs, which are biological strain receptors. This study includes (I) the development of techniques for measurement, (II) an anatomical and biomechanical investigation of the tibia-metatarsus joint of spiders, (III) the measurement of cuticular strains developed by external and internal forces in tethered theraphosids (Avicularіidae), and (IV) the measurement of strain in the legs of freely moving animals.

I. Methods of measurement. The following techniques were developed for the measurement of loads and the resulting strains in the exoskeleton of tethered and freely moving spiders; they are applicable to other arthropods as well.

1. Force: Miniature force transducers (Fig. 1), consisting of bronze springs with strain gauges attached to them, allowed the measurement of point-forces in the tethered animal. Technical data: weight 9 g; sensitivity 2.0 mV/N; stiffness 0.746 mm/N; natural frequency >300 Hz.

The force plate (Fig. 2), used for experiments with freely moving animals was suspended by bronze springs, so that vertical and horizontal components of the ground reaction force could be measured separately. Technical data: platform diameter 50 mm; crosstalk and dependence on the point of application <10%; sensitivity 0.3 mV/N/V; horizontal 0.07 mV/N/V; natural frequency >1 kHz.

2. *Pressure:* Miniature pressure transducers (Fig. 3), consisting of a copper-beryllium membrane with an attached strain gauge rosette, were designed to measure the hemolymph pressure in both tethered and freely moving animals. Technical data: diameter 4 mm; weight 0.7 g; volume displacement 3.8 mm^3/MPa; sensitivity 7.6 mV/MPa/V.

3. *Strain:* Miniature strain gauges (MA XX 008 CK 120) were glued onto the cuticular surface, previously roughened by scouring powder, and gave reliable measurements for up to four months. Owing to the reinforcement of the cuticle (Young's Modulus of the tibia of *Cupiennius:* 18 GPa) by attaching the strain gauge the strain readings were lowered by approximately 10%.

II. Structure and mechanics. The tibia-metatarsus joint of spider legs is a hinge joint with a dorsal axis (Fig. 8). There are no extensor muscles and the antagonizing agent of the flexor muscles is the hemolymph pressure. Moments, joint forces, and strains in the tibia, given by internal and external parameters, were calculated using anatomical data from this joint. The following points were considered:

1. The tibia is almost completely filled with *muscles* (Fig. 10). In contrast to theraphosids (Avicularіidae), muscle arrangement and the joint structure in *Cupiennius* are anteriorly and posteriorly asymmetrical. The arrangement of muscle fibres allows all the fibre forces to be resolved along the centre of gravity from the surface of muscle attachment and thus eases the calculation of moments and forces.

2. *Lacunae* in between the muscles (Fig. 11) form definite channels for the transportation of the hemolymph within and in between the leg segments.

3. Like the muscle forces, the *hemolymph pressure* produces torques around fixed joint axes. This is most effective at specialized joints with axes of

* Present address: Harvard University Concord Field Station, Old Causeway Road, Bedford, MA 01730, USA

rotation located dorsally. However, hemolymph pressure can induce torque at almost every joint in the legs of arthropods. The activity of muscles that run through the joints diminishes the torques generated by hemolymph pressure not only by their antagonistic arrangement but also by reducing the effective area on which pressure is applied.

4. Longitudinal stresses in the *joint membrane,* which might affect extension, are reduced by bellow-like folding (Fig. 12).

5. The *joint forces,* determined by muscle forces, hemolymph pressure and the ground reaction force were calculated (Fig. 13). Joint forces are reduced by the simultaneous activity of muscle forces and hemolymph pressure.

6. *Strains* in the tibia are predicted to reach values of up to 6 με/mN. Using the calculated joint forces, and simple mechanical models, the load conditions for adequate stimulation of the slit sense organs (compression) at the joint region, were predicted.

III. Strains developed by external and internal forces. Cuticular strains in the tibia of theraphosids, which result from loading the distal metatarsus in the axial, lateral, and dorsoventral directions, respectively, were measured at the sites of the lyriform organs located near the tibia-metatarsus joint. From these values the strains developed under any force applied to the leg tip can be calculated.

1. *Axial load* (z'; Fig. 17): The mechanical sensitivities (strain/force) of the lyriform organs are low (<0.8 με/mN) and depend strongly on the tibia-metatarsus angle, α. The sensitivities of all organs are small if the joint is extended, i.e. the tibia-metatarsus angle corresponds to its standard value during slow locomotion. They are large if the joint is flexed. Applying the same load, strains developed at the site of the organ *VS5* located on the ventral surface of the tibia have the same amplitude but opposite sign (−compression, +dilatation) than those developed at the site of the organs *HS8, HS9,* and *VS4* at the lateral aspect of the tibia.

2. *Lateral load* (y'; Fig. 18): Mechanical sensitivities reach values up to 10 με/mN (*HS8*), and sign and amplitude of the sensitivities strongly depend on the tibia-metatarsus angle, α. Again, the organ *HS8* is insensitive to load when the joint is extended.

3. *Dorsoventral load* (x'; Fig. 19): When loaded by internal forces (muscle forces and hemolymph pressure), mechanical sensitivities up to 20 με/mN were found. In general, the strains correlate well with the forces induced at the metatarsus tip. Muscle forces induce compression at the organs *HS8, HS9* and *VS4*. The organ *VS5* is compressed by the antagonistic hemolymph pressure.

IV. Strains in freely moving animals. Strains developing during slow locomotion were measured in the cuticle of the walking leg of theraphosids at the site of lyriform slit sense organs.

1. *Comparison among different organs at the second leg:* Strain amplitudes recorded from the regions of the various organs on the anterior and posterior aspect of the tibia vary only between 13 and 20 με (Fig. 28). The time courses, however, are different; minimum strain occurs during different stages of the leg's stepping cycle (Fig. 29). For example, the organ *HS8* on the posterior aspect of the tibia is compressed (i.e., stimulated) during the power stroke, while the organ *VS5* on ventral aspect is compressed during the return stroke.

2. *Comparison with other sites:* The organs are not located at sites where exceptionally high strain values are occurring. Strain values measured at the dorsal tibia parallel to its long axis were significantly higher (ca. 38 με) than in the region of the organs (Fig. 28).

3. *Comparison among different legs:* Within the same organ the strain time relationships are similar. However, strain amplitudes increase significantly from the first to the fourth leg (Figs. 30, 31). The low value measured at the first leg is due to a lower ground reaction force. The increase from the second to the fourth leg can be attributed to a corresponding increase in torques with respect to the tibia-metatarsus joint.

4. *Influence of mechanical parameters:* The strain amplitude, calculated for the organ *HS8* (4th leg) from the ground reaction force using the proper mechanical sensitivities is in good agreement with the measured value (Figs. 34, 35; Table 2) and can be mainly attributed to muscle forces.

Introduction

This biomechanical investigation was begun to elucidate the mechanical aspects of stimulation in natural strain detectors, i.e. the slit sense organs, which are embedded in the spider cuticle (review: Barth 1981). The exoskeleton does not simply carry these organs but serves as an auxiliary struc-

ture for them (Barth and Blickhan 1984). In principal, any event generating a mechanical load and thus a deformation of the skeleton can be monitored by these receptors. The special, very consistent location of slit sensilla in the respective skeleton part suggests, however, that the mechanical transformation of load into strain is very sensitive to the respective site under consideration.

From behavioural experiments on organs located at the tibia-metatarsus joint and metatarsus-tarsus joint of the hunting spider *Cupiennius salei*, we learned that adequate loads may be generated internally, as during kinesthetic orientation (Seyfarth and Barth 1972), or externally via vibration, as during prey capture (Hergenröder and Barth 1983). Electrophysiological experiments demonstrated, that one organ alone is able to respond over an extraordinarily wide loading range (Bohnenberger 1981). At high loads the organs at the tibia-metatarsus joint elicit protection reflexes at the next proximal joint to avoid overloading (Seyfarth 1978a).

What strain amplitudes are induced by natural loads at the site of the strain detectors? How is load transformed to deformation at the organs' site? Are different organs specialized for certain loads by their special location in the exoskeleton? We tackled these questions in four major steps: I – development of specific methods of measurement, II – anatomical and biomechanical analysis, III – measurement of strain under controlled conditions in a tethered animal, and IV – measurements on freely moving animals.

In the first step (Chapter I) we developed methods to measure loads as well as the induced strains. The only method available to measure the low strain values expected during slow locomotion of freely walking spiders was to attach micro-miniature strain gauges. The application techniques resemble those developed for strain gauge measurements on the endoskeleton of vertebrates (Lanyon 1972; Barnes and Pinder 1974; Bagott et al. 1981), but had to take into account the small dimensions of a spider leg.

The quantification of the load condition in the skeleton necessitated the measurement of reaction forces and hemolymph pressure, which is an important parameter in the spider leg. Consequently a miniature pressure transducer was developed allowing measurements on legs during locomotion. A force plate was designed for measurements of the ground reaction force vector induced during free locomotion.

The second part (Chapter II) provides the anatomical background necessary for execution of the strain and load measurements. Selective stimulation of certain muscles, for example, depends on knowing exact muscle arrangements (compare Parry 1957), and reliable pressure measurements depend on information on the dimensions and positions of the lacunae.

In addition, this part gives a biomechanical interpretation of the main findings, such as calculation of moments and forces produced by muscle action and hemolymph pressure, and their interaction with the ground reaction in the production of joint force. The latter is closely related to the strain measured under different load conditions at the site of the slit sense organs.

The complex loading conditions of the tibia-metatarsus joint of spiders and the location of the slit sense organs in the distal tibia allows only rough estimates of strain values at their site. In the third part (Chapter III) we present direct measurements of these strains under controlled conditions on tethered animals. These measurements enabled us to determine the contribution of special mechanical parameters like hemolymph pressure and muscle forces and, by proper selection of load conditions, to predict strain induced during free locomotion (see Chapter IV).

Beyond its biomechanical relevance, the knowledge of naturally occurring loads and their temporal relationship to the stepping cycle is important to understand the information given to the central nervous system by the biological strain receptors. In the fourth part (Chapter IV) we present direct measurements on freely moving spiders. These include strain measurements as well as measurements of ground reaction force, hemolymph pressure and leg kinematics to quantify the load conditions.

I. Methods of measurement

In this first part we introduce the basic methods of measurement necessary to quantify the small surface strains expected in the exoskeleton of spiders during slow locomotion, as well as the methods used to measure load parameters, i.e. ground reaction force and hemolymph pressure. There are no similar experiments published for arthropods.

1 Measurement of mechanical parameters

1.1 Force

In order to measure forces in tethered animals, induced during the deflection of a leg, a simple

low cost *miniature force transducer* was developed. It consists of a beam of spring-quality bronze, or a copper-beryllium alloy (Deutsche Beryllium-Gesellschaft, Oberursel/Ts) with a foil strain gauge (FLG-02-11, TML; Fig. 1) attached to it. The dimensions used were calculated according to a formula used in beam theory (Szabo 1975):

$$s = 6 \cdot L \cdot F / b \cdot h^2 \cdot E \quad (1)$$

s, strain in the clamped region; b, h, L, bar width, height and length, respectively; E, Young's Modulus; F, force applied at the bar end.

The natural frequency (f_0) of a clamped beam with the mass m attached to its free end follows the equation (Szabo 1975):

$$f_0 = 1/2\pi(1296 \cdot E \cdot b \cdot h^3/12 \cdot K \cdot 14\,(104 + 405 \cdot m/K \cdot L))^{1/2}, \quad (2)$$

K, mass of beam/length.

From this the proper dimensions were calculated ($b = 3$ mm, $L = 10$ mm, $h = 0.3$ mm) with the following consequences:

a) A small transducer mass of 8.7 g could be employed. This meant that up to 10 Hz the frequency characteristics of the feedback controlled electrodynamic vibrator (Bohnenberger 1979) were not affected by the attached transducer.

b) The sensitivity (2.02 mV/N/V) and stiffness (0.746 mm/N) of the transducer could be adjusted to the stiffness of the object undergoing measurements.

c) An adequately high natural frequency (> 300 Hz) was achieved.

To measure the ground reaction force vector induced by the leg of the freely moving animals a *force plate* was developed. It consists of two plastic rings, which are connected by four bronze springs and fastened to the base with four additional springs (Fig. 2a). The upper ring serves as a platform (diameter: 50 mm) onto which the animal steps when walking along the track. The wiring and arrangement (Fig. 2b) of the strain gauges (FLG-02-11, TML) glued onto the springs (E-Bond 610, Vishay) allows the simultaneous and independent measurement of the three force components Fx, Fy, Fz. Sensitivities: Fz, vertical: $3 \cdot 10^{-4}$ mV/N/V and Fx, Fy horizontal $7 \cdot 10^{-5}$ mV/N/V. Crosstalk and point of application of the force account for an error of less than 10%. The natural frequencies are greater than 1 kHz.

1.2 Pressure

Requirements. Measurement of the hemolymph pressure requires a transducer with the following

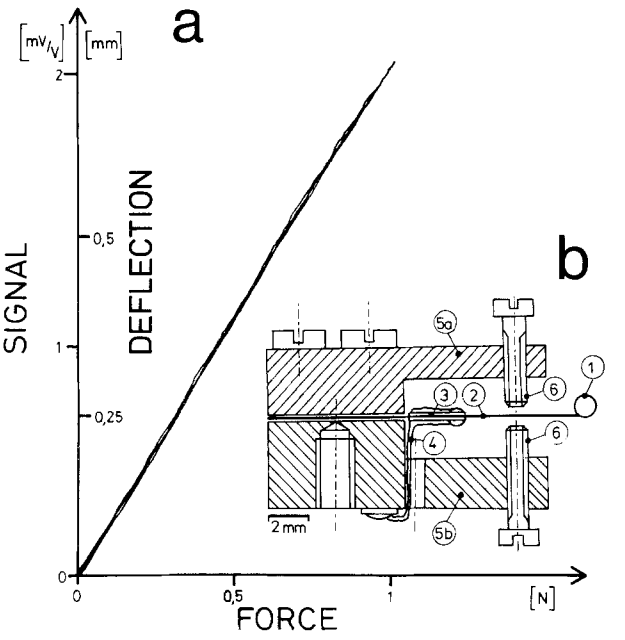

Fig. 1a, b. Miniature force transducer for measurement of the forces applied to the spider leg. **a** The calibration characteristics consist of an inner (rate: 30 mN/s) and outer (rate: 1 N/s) hysteresis loop (<1%). x-axis: force applied to the transducer's tip; y-axis: output signal/supply voltage. **b** Cross section of force transducer. *1* hook for coupling; *2* bar spring; *3* strain gauge; *4* wires; *5* brass clamps; *6* deflection limits

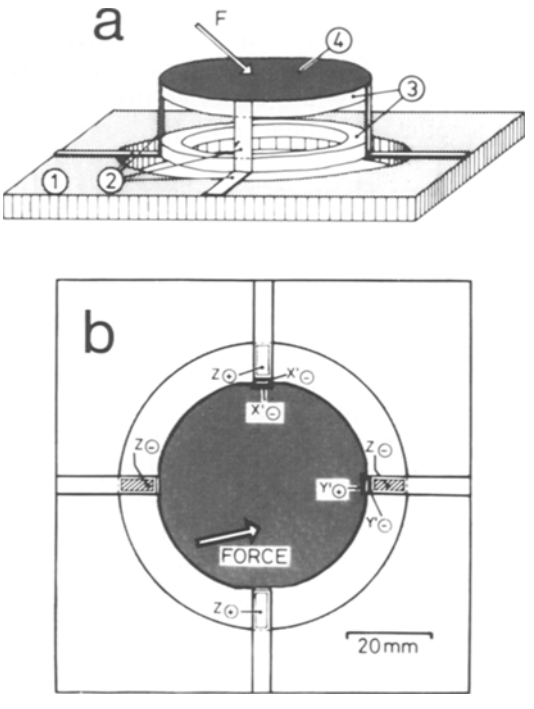

Fig. 2a, b. Force plate. **a** Perspective view. *1* ground plate; *2* bronze springs; *3* plastic rings; *4* cardboard; *F* applied force. **b** Vertical projection and wiring of the strain gauges. *z* strain gauges for measurement of the vertical force component; x, y horizontal force components; +, − wiring in a wheatestone bridge (*z*: full-bridge, *x*, *y*: half-bridge)

properties: (a) the diameter of the transducer tip should be similar to that of the blood channels in the leg (see Chapter II), i.e. smaller than 1 mm. (b) The transducer must be neither too heavy nor too bulky, so that the freely running animal is hampered as little as possible (weight of a tarantula's leg: ca. 0.6 g). (c) The transducer must be stiff, i.e. the volume displacement has to be as small as possible. Failing this, a considerable proportion of the hemolymph fluid must be branched to the transducer. This would lead to a delay of the hemolymph pressure in the region of the joint, or, in the case of a short pulse, to a decreased pressure value (see Chapter II). (d) The maximum pressure the transducer has to cope with can reach up to 70 kPa.

Design: The basic transducer element developed consists of a copper-beryllium membrane attached to a ring of brass (Fig. 3). The displacement of the membrane by increased pressures is measured with a strain gauge rosette. The requirements of small volume displacement, high sensitivity, as well as small dimensions mean miniaturization of this basic component. The smallest commercially available membrane rosette (diameter: 2.3 mm, FAE-S4-09-12-S6, Baldwin) determined the size of the transducer. The following formulae (technical note 129-3; Vishay) form the basis for the choice of membrane material and its thickness. The membrane thickness, T [mm], is given by:

$$T=(0.82\cdot 10^3\cdot P\cdot r_0^2\,(1-\mu^2)/E\cdot e_0)^{1/2}. \quad (3)$$

The maximum membrane deflection, D [mm], is given by:

$$D=3\cdot P\cdot r_0^4\,(1-\mu^2)/16\cdot t^3\cdot E, \quad (4)$$

P [MPa]: maximum pressure; r_0 [mm]: membrane radius; e_0 [mV/V]: maximum output voltage per unit input voltage; μ Poisson's ratio.

With highly elastic copper-beryllium membranes, 20 µm thick (Deutsche Beryllium-Gesellschaft, Oberursel/Ts.), the design requirements can be fulfilled. A transducer built in this way and with the rosette glued to the membrane with hot, precipitation hardened adhesive (E-Bond 610, Vishay) has a linear working range (without hysteresis) up to 100 kPa (Fig. 3c).

A typical sensitivity value, measured with a mercury differential manometer, is 3.76 mV/MPa (bridge supply 0.5 V) and the volume displacement amounts to ca. 0.05 mm^3/100 Torr = 3.75 mm^3/MPa. The natural frequency of a transducer filled with Ringer's solution (see below) is higher than 300 Hz.

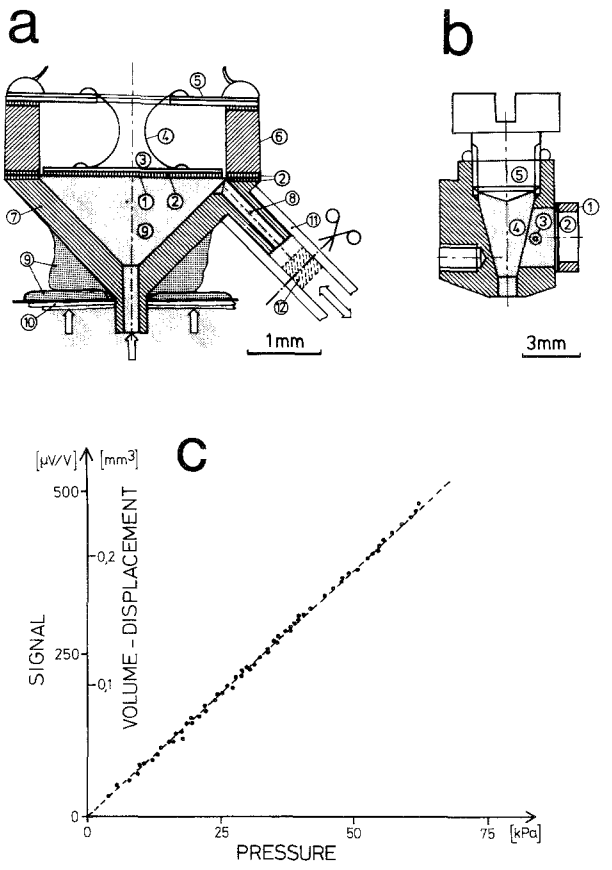

Fig. 3a–c. Transducer for the measurement of hemolymph pressure. **a** Miniature transducer for measurements in freely walking animals. *1* membrane; *2* adhesive; *3* strain gauge rosette; *4* wires; *5* cover; *6* ring of brass; *7* funnel filled with Ringer's solution; *8* reference channel; *9* wax colophonium; *10* cuticle; *11* plug for sealing after the reference tube (*12*) is cut; arrows: hemolymph pressure. **b** Transducer for measurements on tethered animals. *1* brass ring with membrane (*2*); *3* reference channel; *4* funnel filled with Ringer's solution; *4* locking screw; *5* cuticle; **c** Calibration

Mounting. In experiments on freely moving animals, the previously described basic transducer element is mounted on a funnel (tip diameter 0.5 mm; Fig. 3a). Ringer's solution can be passed through a reference channel. The mass of a transducer together with the funnel is ca. 0.7 g and, indeed, hardly hampers freely moving bird spiders.

In experiments on tethered animals the transducer mass is immaterial. Thus, to facilitate application, a bigger funnel with the basic transducer element mounted at its side was used (Fig. 3b). After dry sealing of the transducer at the cuticle surface, the blood channel could be opened by drilling a hole into the cuticle through the funnel filled with Ringer's solution.

Measurements. In order to find a suitable site, pressure measurements were taken simultaneously

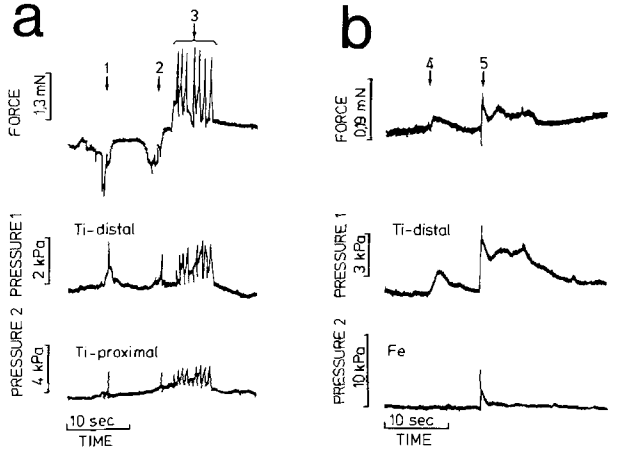

Fig. 4a, b. Hemolymph pressure at different sites of the leg of the spider, *Cupiennius salei*, and force developed at the metatarsus tip. **a** The pressures measured proximally and distally in the dorsal hemolymph channel of the tibia (see Chapter II) agree with repect to amplitude and time course. The first pressure pulses (1, 2) are induced by the activity of flexor muscles whereas the following series (3) is hardly influenced by muscles in the tibia. **b** The pressures measured in the femur (*Fe*) differ from those in the tibia (*Ti*). Despite of similarities of the time course of pressure in the tibia and force developed at the metatarsus tip, again, the influence of flexor muscles is seen (4, 5)

from several points on the leg of the hunting spider *Cupiennius salei*. The hemolymph pressure in the dorsal blood channel (see Chapter II) corresponds to the pressure measured in the distal joint region (Fig. 4a). There are amplitude and time differences in pressures outside the channels and in different leg segments (Fig. 4b). When the spider struggled, peak pressures of 70 kPa were measured, and the highest pressure value, recorded during autotomy of a leg, was 130 kPa.

The simultaneously measured change in hemolymph pressure and torques over time show that there are not only periods with alternating extensions and flexions, but also periods when there are no torques at all, due to simultaneous compensating effects of hemolymph pressure and muscle force.

1.3 Strain

Method. For recording cuticular strains in the region of slit sense organs, foil strain gauges were used and the following advantages discerned:

a) Using foil-strain gauges the local discrimination of strain gradients is limited by the smallest commercially obtainable grid-area (MA XX 008 CK 120, grid: 0.2×0.25 mm, or EA XX 016 CK 120, grid: 0.4×0.45 mm, Vishay). This area is of the same order of magnitude as the slit sense organ's size (ca. 0.1×0.3 mm), so that measurements with sufficient space resolution are possible.

b) The foil thickness is less than half the wall thickness of the tibia (ca. 90 µm). Young's Modulus of the tibial cuticle (ca. 18 GPa) is more than triple that of the gauge foil. Under these conditions, the measured values can be expected to be up to 25% too low (Müller 1971; Glücklich 1976). This seemingly large inaccuracy is justifiable, because this technique is the only one which allows the measurement of the amplitude and time course of strains in the exoskeleton of freely moving animals (see Chapter IV)).

c) The strain gauge, with its small mass (ca. 0.6 mg) does not hinder a freely moving animal.

d) Using strain gauges with short grids, displacements in the cuticle of less than 1 nm can be resolved by conventional signal conditioning.

Application. The strength of adhesion of the strain gauge depends mainly on the surface preparation, which was done in 4 steps: (a) Removing of the cuticular hairs, using a scalpel. (b) Slightly dissolving the surface layer with ethanol. (c) Roughening the surface with scouring powder. (d) Cleaning of the surface with ethanol.

A wired and trimmed strain gauge was then glued to the surface with a quick setting adhesive. Such applications allowed repeatable measurements to be made for up to four months. The animals exhibited no sign of experiencing interference and even ecdysis was unaffected.

Accuracy. Both to control the accuracy of the strain readings and to determine Young's Modulus, displacement readings were taken using axial pressure loaded tibiae of the hunting spider, *Cupiennius salei*. The ends of the tibiae were cast with dental cement (Fixodent, De Trey) in the jointed region. The loads applied to these ends were measured by a force transducer (FT 03C, Grass) and the shortening of the probe was measured by a linear transformer (TW 10B, TWK). The strains directly measured by strain gauges (s_G), and those calculated from the displacement (s_D), deviate by only 10% ($s_G/s_D = 0.9 \pm 0.4$ SD, $n = 16$, $N = 2$). This deviation is due to the stiffening of the cuticle by the application of the strain gauge.

Temperature. Temperature variations can induce changes in the strain signals due to the differences in the coefficients of thermal expansion of the materials used. When calibrated, the cuticle-strain gauge system has a temperature coefficient of 13 µε/°C. Temperature variations, during an exper-

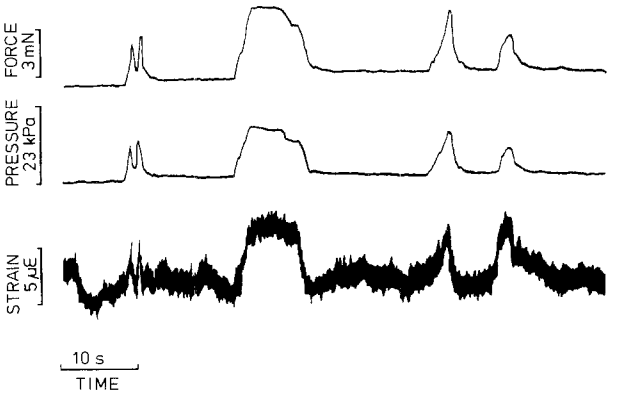

Fig. 5. Simultaneously measured force at the metatarsus tip, hemolymph pressure in the proximal tibia, and strain in the region of the 'lyriform' organ HS9 at the posterior aspect of a tarantula's tibia. An artificial pressure was applied via the reference channel of the transducer (Fig. 3). Strain, pressure, and force display similar time courses

iment, were limited to about 0.1 °C by thermal insulation. In every case, the temperature was continually recorded and data were only used when there were stable temperature conditions. In experiments on tethered animals, necessitating stable conditions for up to 10 min, the cage temperature was controlled and stabilized at 28 °C. To avoid a signal drift, induced by local production of Joule's heat, the supply voltage for the strain gauge, should not exceed 0.5 V (Vishay Micro-Measurements, technical note-127-3).

Signal processing. The output signal of the modified conditioner (2100, Vishay) was filtered (low pass, characteristic: Bessel, Tschebyschew, Butterworth, critical; cut off frequency: 80, 300, 1,000 Hz; Möller, own development). A built-in differential amplifier (amplification: 1, 3, 10, ..., 1000; common mode rejection: 80 dB) raises the low output voltage to a level, which allows storage of the signal with the aid of an fm-taperecorder (Analog 7, Philips). Strain amplitudes down to several με can be registered. Strains up to 6 με/mN are expected theoretically.

Measurements. In the tibia of tethered spiders, strains of up to 100 με were measured. In most cases, the time courses of both force and strain are similar (Fig. 5). Creep effects are negligible, even for static loads.

2 Discussion

Today, strain gauge techniques are widely used in the measurement of mechanical parameters in living animals. The particular value of the methods described here is their close adaptation to their special purposes in our biomechanical study on spiders (Table 1).

Table 1. Own developments contrasted with transducers described in literature and those commercially available. The data from the types selected are closest to our various requirements. Transducers we have developed have the advantages of: low cost, close adaptation to specific situations and their drive by strain gauge conditioners. In experiments where animals are allowed to move freely robustness is an important requirement, not fulfilled by the pressure transducers commercially available

	Own development	Literature	Commercial	
Miniat. Force		(Allan et al. 1980)	(BG, Kulite)	
Sensitivity	2	9.5	250	mV/N/V
Stiffness	1.3	50	5	N/mm
Natural frequency	>0.3	1.35	7	kHz
Weight	9	–	1	g
Length	15	50	12	mm
Force plate		(Heglund 1981)	(9067 Kistler)	
Sensivity	0.3	0.15	(8 pC/N) threshold: 10 mN	mV/N/V
Natural frequency	>1	0.17	30	kHz
Cross talk	<10	5	5	%
Dependence of force appl. site	<5	3	1	%
Length	50	250	50	mm
Pressure		Transducers are not applicable on freely moving spiders	(CQ080, Kulite)	
Sensitivity	8			mV/MPa/V
Volume displacement	4		380	mm/MPa
Natural frequency	>0.3		1.5	kHz
Weight	0.7		230	g
Diameter	4		0.2	mm
	tip: <0.5		0.7	

Miniature force transducer. More sensitive and stiffer transducers with semiconducting strain gauges have been described elsewhere (Allan et al. 1980) or are commercially available (BG, Kulite). Our own development has produced a simple low cost transducer with small size and high robustness. In experiments with living animals high over-

loads could be expected during struggles; but by selecting the proper bar material and dimensions the sensitivity and the mechanical impedance of the force transducer can be adjusted to the specific stiffness of the object under investigation.

Force plate. The thresholds of the force plates commercially available are much too high to sensitively measure small ground reaction forces (40 mN pp.) such as those generated by a large tarantula's leg. The force plate described recently by Heglund (1981) is too large, and measures only one horizontal force component.

The force plate developed for measurements on tarantulas and hunting spiders has a high resonance frequency. Moreover, signals from the separate force components are independent of the point of force application and have a low crosstalk, which is achieved without any mathematical processing.

The method to measure the ground reaction force optically, by using a photoelastic substrate (Harris 1978), has the advantage that the forces at the tip of the different legs can be measured simultaneously and registrated optically together with leg kinematics (Arcan 1982). However, until now, this technique has not allowed a clear separation of the different force components.

Pressure transducer. Notable properties of the developed transducer are its low mass, low volume displacement and high resonance frequency. Other transducers used for the measurement of hemolymph pressure in arthropods (Bayer 1968; Stewart and Martin 1974; Slama 1976) are relatively large and therefore have to be connected, via fluid filled tubes, to the animal's hemolymph. In measurements on unrestrained animals, this leads to low natural frequencies and artifacts caused by movements.

The most suitable transducer commercially available (CQ 080, Kulite) is delicate and can not be implanted repeatedly. The high failure rate of its lead wires especially, does not allow experiments on freely running animals. Moreover, the construction of an adapter consisting of a membrane and a funnel is necessary to protect its surface from attack by the hemolymph and diminishes the advantage of its small size.

With respect to the pressure values reported for insects (see Chapter II), the sensitivity of the developed transducer (7.6 mV/N/V) is too low.

Strain measurement. Strains in the exoskeletons of arthropods can be measured by miniature strain gauges. The stiffening of the cuticle introduced by the strain gauge leads to a systematic deviation of about 10%. However, at present there are no alternative techniques with the same advantages regarding accuracy, resolution, robustness and low mass.

Other techniques fail because of their low resolving power (piezo ceramiques), their effects on stress in the region of the organs (semiconductor strain gauges), and their inapplicability for measurements on moving objects (optical techniques).

For investigations on the endoskeleton of vertebrates, foil strain gauges have already been successfully applied (Roberts 1966; Lanyon and Smith 1969; Cochran 1972; Carter 1978; Bagott et al. 1981), and there is great similarity between previous techniques and our own independently developed technique. The differences lie in the size of the investigated objects and in some details in surface preparation (vertebrates, Wright and Hayes 1979; arthropods, Blickhan and Barth 1979; Blickhan et al. 1982). Because of the high stiffness and large dimensions of strain gauge rosettes (Carter 1978; Lauder and Lanyon 1980) used in the determination of the main strain direction, they can only be employed on thick and extended parts of the skeleton of spiders and insects.

Cuticle. As a prerequisite for using strain gauges, the stiffness of the cuticle must be higher than that of the gauge foil. The value of Young's Modulus, determined for the cuticle of the tibia of *Cupiennius salei* under pressure load, is one of the highest known for any cuticle (survey: Hepburn and Joffe 1976) and resembles the value for bone (survey: Yamada 1970; Carter 1978). The Young's Modulus probably varies within different regions of an appendage, therefore, strain measurements should be supplemented by determinations of local mechanical properties. According to present theory (Vincent and Hillerton 1979; Elliot 1981) the stiffness of the cuticle depends mainly on the water content, which in some cases is known to be under hormonal control. Local mechanical anisotropy in the surface plane can be excluded because of the helicoidal, isotropic microfibre arrangement in the leg cylinder of *Cupiennius* (Barth 1973).

II. Structure and mechanics

Execution and interpretation of strain measurements require detailed knowledge of the investigated structures and their mechanical relationships. In the following paragraphs we will discuss the function of elementary mechanical structures in an arthropod leg joint in general, and of the

spider's tibia-metatarsus joint in particular. Moreover, it will be shown how these structures interact in the production of strain in the spider's tibia.

1 Material and methods

Animals. Most of the anatomical investigations were done with adult females of the Central American hunting spider *Cupiennius salei* Keys. From our own stock (Melchers 1963; Barth and Seyfarth 1979). Tarantulas (wild caught: subfamily Aviculariidae, classified as *Aphonopelma seemanni, Aphonopelma* sp., *Brachypelma* sp., *Tapenauchcinus* sp.; verification by C. Valerio, University of Costa Rica) were favoured for strain measurements, because they have larger leg diameters (mean diameter of the tibia of the second leg: 3.4 mm $\pm$ 0.1 SD; *Cupiennius:* ca. 2 mm). During experiments, the animals were blinded with black printing paint to avoid interferences through visual stimuli (Seyfarth and Barth 1972). As far as possible, the same animals were used in both the experiments on freely running and on tethered animals. This enabled us to check the quality of the strain gauge's adhesion and to determine the mechanical sensitivity on the same individual with exactly the same measurement site.

Anatomical investigation. The geometry of the cuticular skeleton was determined using conventional histology. The form and the site of the slit sense organs of bird spiders (*Cupiennius:* Barth and Libera 1970) were studied with the light (squeeze probes) and scanning microscope (S-500, Hitachi). The arrangement of the muscles was investigated using fresh and ethene stained probes.

The following methods were applied for the reconstruction of the hemolymph channels: (a) Observation of the movement of cells beneath the transparent cuticle in animals, two to three months old. (b) Observation of hemolymph coloured by methylene blue injected in the distal leg of adult animals some days after ecdysis. (c) Injection of coloured gelatin (Adam and Czihak 1964), which after cooling permitted the form of the lacunae to be preserved, and the cross sections to be measured.

2 Results

2.1 General results on the 'Bauplan' of arthropod legs

Design of the exoskeleton. The skeleton of arthropods consists of thin walled, tube like cuticular components, connected by joints with surfaces that are much smaller than the limb's cross section. A flexible cuticular joint membrane is spread between the stiff limb segments. In joints with large angles of rotation the membrane is often folded like bellows (Fig. 12).

For animals that move their limbs quickly and with large amplitudes, long and slender legs with most of the mass concentrated proximally are advantagous since they reduce the problem of inertial forces. Thus a large proportion of the muscle mass activating the proximal leg segments, is placed within the body. Joints of several degrees of freedom (ball joints) are located proximally, close to the trunk. Hinge joints are found chiefly in the middle portion of the leg because they do not need muscles for stabilization perpendicular to the main plane of movement. The most distal and often short segment is indeed free of muscles and activated by long tendons. Even when movement can only be actively adjusted in one direction, the distal joint is often of the ball and socket type. Errors in the position of the most distal segment can only lead to small errors in the position of the animal.

Load parameters. Internal forces developed by muscles and hemolymph pressure allow for active and controlled deflections of leg segments.

1. Muscle forces (Fig. 6): The moment $\vec{M}_m$ is determined a) by the magnitude and direction of the muscle force vector ($\vec{F}_m$) which in turn depend on cross-section, fibre direction and recruitment, and b) by the location of the centre of gravity of the muscle attachment ($\vec{r}_s$) with respect to the rotational axis of the joint:

$$\vec{M}_m = \vec{s} \times \vec{F}_m. \tag{5}$$

2. Hemolymph pressure (Fig. 6): The moment produced by the hemolymph depends a) on the pressure amplitude (P), (b) the magnitude of the 'effective area' (A), (c) its orientation ($\vec{n}$) and d) the position of its centre of gravity, with respect to the joint axis ($\vec{r}_s$):

$$\vec{M}_P = P \cdot A(\vec{r}_s \times \vec{n}). \tag{6}$$

A, $|\vec{r}_s|$, and therefore the torque developed from a particular pressure can be lowered by activating muscles passing through the effective area.

Equation (6) is based on the integration of the torques developed by the hemolymph pressure acting on every differential element of the effective area. Another Eq. (7) can be deduced by using the law of energy conservation. The energy needed to rotate the leg by a differential angle $d\Theta$ during constant pressure (P) is required to displace the differential volume dV:

$$M \cdot d\Theta = P \cdot dV, \text{ and } M = P \cdot dV/d\Theta. \tag{7}$$

Parry and Brown (1959a) verified this equation for the spider leg experimentally, but without explicit notation. The Eqs. (6, 7) are related by Guildin's rule.

In general, in arthropod joints torques can be produced by hemolymph pressure if the centre of gravity of the effective area is not located at the rotational axis of the joint (Eq. 6) and if the internal volume of the leg can be changed by rotating the limb (Eq. 7).

The internal forces developed by the animal,

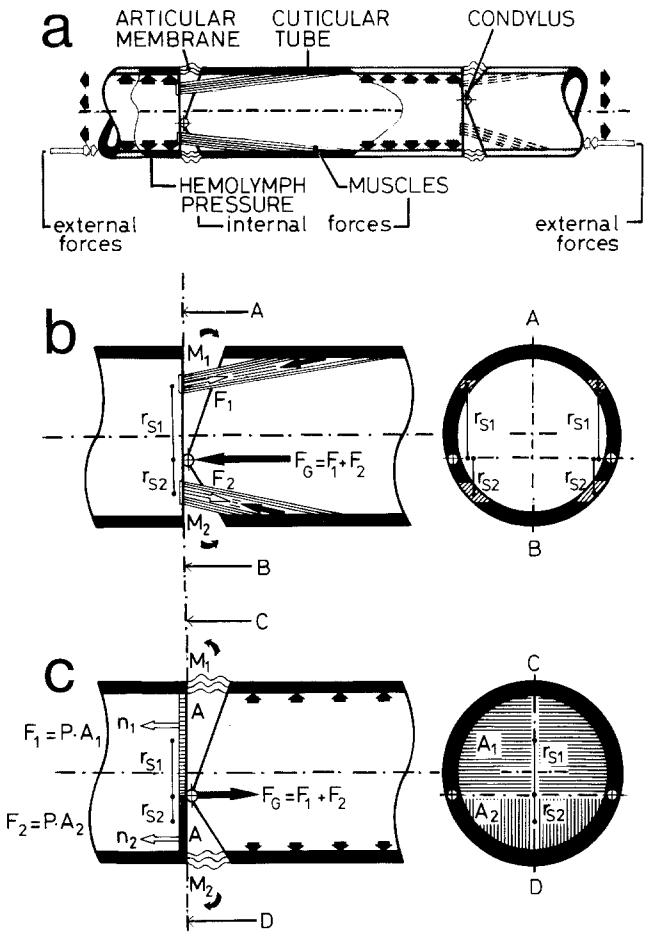

Fig. 6a–c. Mechanical 'Bauplan' of arthropod legs: **a** Arthropod legs consist of tube like segments, which are connected by joints with contacting surfaces small with respect to the segment's cross section. External (⇨) and internal (◗) forces (hemolymph pressure and muscles) determine the loading condition of the segments. **b** Torques developed by muscle forces. The vectors of the muscle forces (F_i, i=1,2⇨) apply in the centre of gravity (r_{si}) of the attaching surfaces developing the torques M_i (↷). **c** Torques developed by hemolymph pressure. The pressure (P) developed by the hemolymph acting at the effective surface (A_i, orientation n_i, center of gravity r_i) induces the torque M_i (↷). ◗ forces developed at the segment under investigation; F_G resulting joint force

have to cope with external forces, such as gravity or the ground reaction force. Torques ($\vec{M}_G$) generated by gravity depend on (a) the location of the centres of gravity with respect to the rotational axis of the joint ($\vec{r}_s$), (b) limb orientation with respect to the vertical, and (c) on the weight of the segments ($\vec{F}_G$). Similarly, torques ($\vec{M}_A$) developed by the ground reaction force depend on the distance of the leg's tip from the rotational axis of the joint ($\vec{r}_A$) and on magnitude and direction of the force vector ($\vec{F}_A$).

$$\vec{M}_A = r_A \times F_A. \quad (8)$$

Joint forces. Consideration of internal and external factors, allows joint forces to be calculated at equilibrium conditions, i.e. when resolved force and torque are zero.

The joint force is minimum when the ground reaction force is directed almost parallel to the distally adjacent leg segment, and active parameters (muscle forces and hemolymph pressure) do not have to compensate for torques developed. In contrast, joint forces are many times greater than external forces, if internal forces compensate for torques developed by components of the ground reaction forces, not aligned with the adjacent segment.

The features described generally resemble those found in the vertebrate joints, but there remain some important differences. In vertebrates, stabilization of a joint by antagonists acting simultaneously leads to high joint loads which must be distributed over a relatively large joint surface to avoid damage. In arthropods and especially in spiders, the forces in a joint can decrease to zero, despite the activity of muscles and the presence of hemolymph pressure. The pressure load, induced at the joint by muscles, is compensated by the tension load generated from the antagonistic hemolymph pressure. Consequently, loads acting on relatively small joint surfaces vanish.

2.2 *Functional morphology of the spider tibia*

The tibia and the tibia-metatarsus joint of spiders were chosen for strain measurements for two reasons: (a) Organs located on the tibia have already been examined with electrophysiological techniques and with model studies (Barth 1981; Barth and Blickhan 1984; Barth et al. 1984); (b) the antagonistic interplay of muscles and hemolymph pressure, at this joint, facilitates the separation of these internal parameters.

Cuticle structure. The tibia of *Cupiennius* is a thin-walled, cylindrical tube (wall thickness ca. 90 µm; exo- and mesocuticle ca. 35 µm, Barth 1973; ca. 2 mm in diameter and 13 mm long). Only in the joint region up to 1.5 mm from the distal end of the tibia is the radial deviation more than 10% from the circular form (Fig. 7).

The tibia-metatarsus joint is of the hinge type (main plane of movement: dorso-ventral), with an axis on the dorsal side (Fig. 8). There are three condyli, and the median one is slightly shifted towards the anterior (ratio of distances to the outer condyles ca. 2:1). The median condylus is not lo-

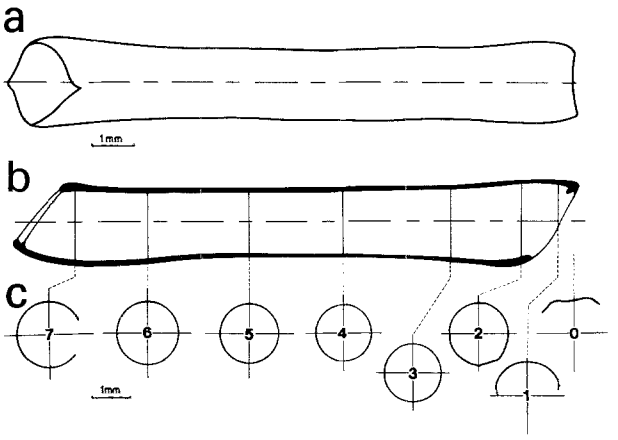

Fig. 7a–c. Geometry of the tibia of *Cupiennius* (to the right: distal end). **a** Dorsal view. **b** Longitudinal section. **c** Cross sections (outer edge). In the middle portion of the tibia the cross sections are circular. Near the joints their diameters are increasing. The cross sections of the tibia are open there (0, 1, 7) due to the obliquely cut ends

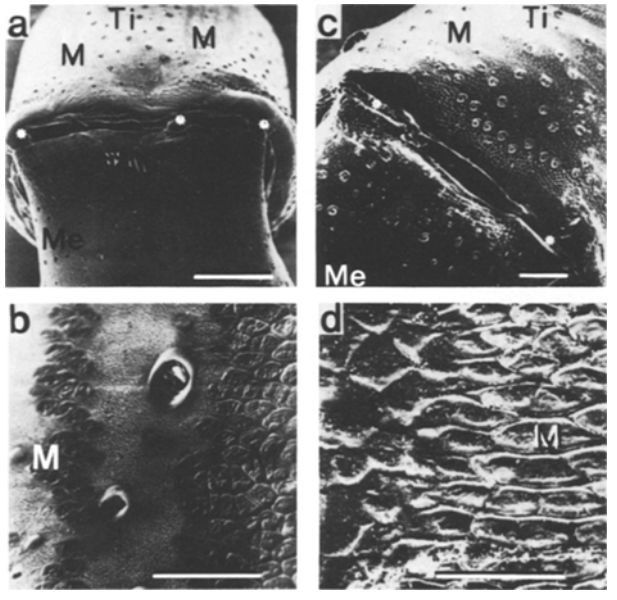

Fig. 8a–d. Tibia-metatarsus joint. *Ti* tibia; *Me* Metatarsus. **a** Joint of *Cupiennius salei;* left side posterior, right side anterior. The three condyles (*) are not arranged on straight line. *M* Muscle attachment site; scale: 500 µm. **b** Edge of a muscle attachment site (detail from **a**; scale: 50 µm). The cuticular surface surrounding the muscle attachment site (*M*) is ribbed. At the sites of muscle attachment there are no hairs. **c** Joint of a tarantula. The two condyles (*) are elongated (scale: 50 µm). **d** Edge of a muscle attachment site (detail from **c**; scale 50 µm); surrounding cuticle is scaley

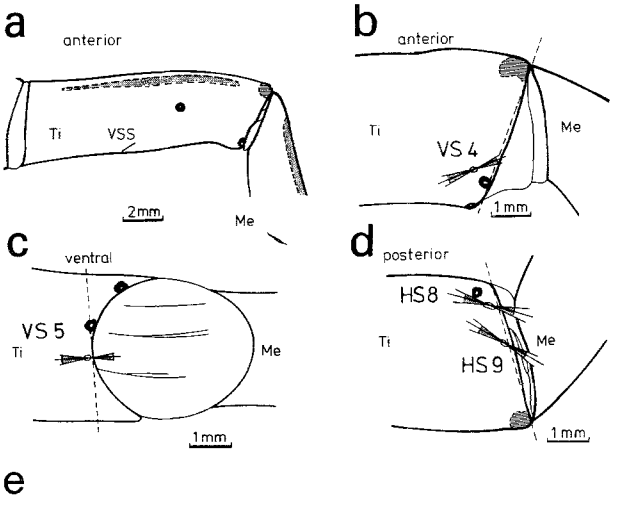

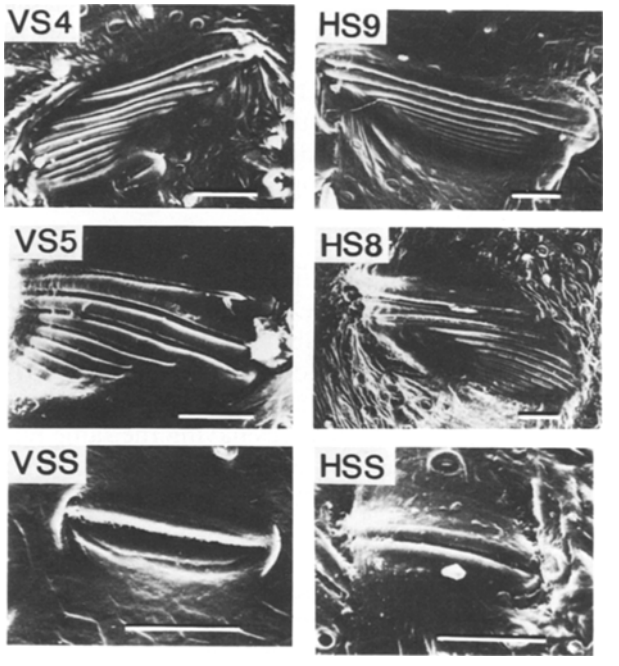

Fig. 9a–e. Location, orientation and shape of the slit sense organs of the tibia (*Ti*) of theraphosids (*Aphonopelma* sp.; nomenclature see Barth and Libera 1970). **a** Single slit (*VSS*) at the anterior aspect. There is a symmetrically orientated slit (*HSS*) at the posterior aspect. **b** Lyriform organ *VS4* at the anterior aspect of the tibia. **c** Lyriform organ *VS5* at the ventral aspect. **d** Lyriform organs *HS8* and *HS9* at the posterior aspect. (⟶ orientation of the organs ±SD; --- reference line; ● condyle region and muscle attachment areas in **a**; ● spines). **e** Scanning electronmicrographs (scales for HS8, HS9, VS4, VS5 50 µm, for VSS and HSS 5 µm)

cated on the axis connecting the lateral condyles; if the metatarsus is flexed the outer condyles are in contact, when extended lateral rotation around the median condyle is possible. The joints of tarantulas do not have such a median condylus.

Slit sense organs. The site of lyriform organs at the tibia-metatarsus joint of theraphosids (Fig. 9) is similar to that of *Cupiennius* (Barth and Libera 1970). The number of slits in an organ is higher in tarantulas, in particular in the organ VS5 at

the ventral tibia, which consists of two slits in *Cupiennius* but eight slits in the tarantula (Fig. 9e). In contrast to *Cupiennius* theraphosids do not have single slits at the dorso-lateral tibia parallel to its long axis. Instead there are two large single units situated ventro-laterally, anteriorly and posteriorly in the middle of the tibia, oriented at about 45° to the long tibial axis.

Muscles. The tibia is almost completely filled with muscles, which all are flexors because of the dorsal axis of rotation (Fig. 10). In between the *Flexor metatarsis longus* (Fl. met. long.) and the *Flexor metatarsis bilobatus* (Fl. met. bil.), another pair of muscles has been found (*Flexor metatarsi accessorius* = Fl. met. acc.) which insert dorsally in the proximal tibia and run to its distal and ventral part where they attach to the tendon of the Fl. met. long. In *Cupiennius* the anterior part of the Fl. met. bil. is larger than the posterior one, as is seen from the different size of the dorsal muscle attachments (see Fig. 8). If the leg is straightened, the larger part pulls on the shorter lever defined by the location of the medium condyle. Again, this asymmetric muscle arrangement is not found in theraphosids.

Independently of the tibia-metatarsus angle, the forces of the muscle fibres of the Fl. met. bil. can be resolved along the centre of gravity of the muscle attachment, distributed over a curvilinear region at the proximal end of the metatarsus. This is due to the parallel fibre arrangement that, during joint rotation, results in fibres having the same relative change of length (law of radii) and the same force, if they are equally stimulated.

Lacunae. During joint rotation, the lacunae in between the muscles, arteries, nerves and the skeleton serve to transport the hemolymph to or from the joint, or to the more distal segments (Fig. 11). This is especially true at a joint, where hemolymph pressure is the only antagonising agent to muscle forces.

In the spider tibia, a dorsal channel in between the flexor muscles supplies the more distal limb segments with hemolymph. Dorsoventral channels branch off laterally from the proximal end of the dorsal channel. They run parallel to the boundaries of the different muscles and empty ventrally into the joint region. The cross-sections and thus the hemodynamic resistances of these channels are varied by muscle contraction. At the proximal end of the metatarsus, muscles form a closed ring, and here it is impossible for hemolymph in the dorsoventral channel to be quickly squeezed into the

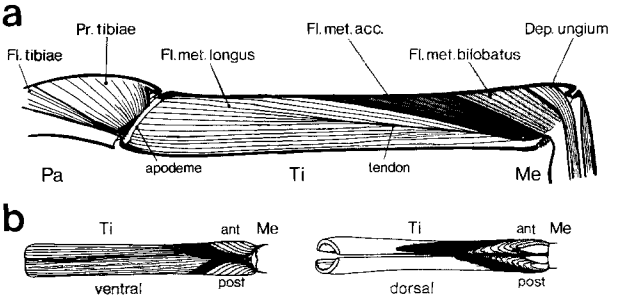

Fig. 10a, b. Arrangement of muscles in the tibia (*Ti*) of *Cupiennius salei*. *Pa* patella; *Me* metatarsus. **a** Longitudinal section. **b** Ventral and dorsal aspect. Muscles from the left (proximal) to te right (distal): *Flexor tibiae, Promotor (remotor) tibiae; Flexor metatarsi longus, Flexor metatarsi accessorius* ▭, *Flexor metatarsi bilobatus promotor (remotor)* ▨, *Depressor ungium*. In contrast to the anterior and posterior asymmetrical arrangement in *Cupiennius* the muscles are arranged symmetrically in tarantulas

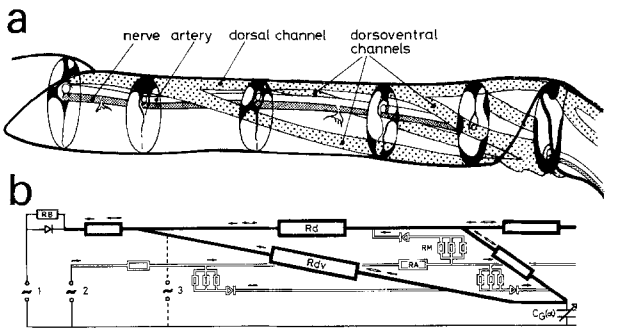

Fig. 11a, b. Lacunae in the tibia of spiders form channels which provide fast transport of the hemolymph during active and passive movement of the joints. Pressure measurements must be done in these channels, because of the volume displacement of the transducers. **a** The dorsal channel, embedded in between muscle attachments provides for a quick supply of the adjacent segments, whereas the dorsoventral channels are closed distally. The course of the channels is simplified (black: original cross sections). **b** Circuit explaining fluid mechanics in the tibia. — supply by arterial hemolymph; ⊣▭⊢ fluid resistances of the arteries (R_A) and the muscular capillaries (R_M); ⊣⊢ valves prohibiting backflow; — lacunae; ⊣□⊢ fluid resistances of the dorsal (R_d) and dorsoventral (R_{dv}) hemolymph channels; ≠ C_G (α) volume displacement of the articular membrane; ⧫ flow direction of the circulation; pumping direction during leg movement; ⊣⊢ valves and resistance (R_B) of the channels in the proximal leg segments; ∿ pressure sources: 1 prosoma, 2 heart, 3 muscles

dorsal channel or the more distal segment. Thus extension can be generated independently from the filling up of more distal segments. On the other hand, a sudden pressure release in the dorsal channel caused by passive extension of the metatarsus-tarsus joint does not lead to a sudden breakdown of torques produced at the tibia-metatarsus joint. Moreover, because of their elasticity, muscle rings and articular membranes are able to store both hemolymph and energy (comp. Sect. 3.1.2).

A rough calculation of the resistance of the channels, assuming laminar flow in tubes (Hagen-Poiseuille) and neglecting the velocity dependence of the viscosity (Charm and Kurland 1972), results in the following values: $R_{\text{dorsal}} = 1.5 \cdot 10^{10}$ kg/s·m^4 and $R_{\text{dorsoventral}} = 2.2 \cdot 10^9$ kg/s·m^4. This allows the whole tibia-metatarsus joint of *Cupiennius* to be filled in $\tau = 1$ ms, if the pressure is raised to 66 kPa. For the pressure measurements, cut-off frequency higher than 50 kHz was estimated (see Chapter I) by considering the flow resistance and volume displacement for the transducer.

Extensions. Muscles running through the joint (Fl. met. bil. and Fl. met. acc.) allow variation in the moment induced by hemolymph pressure. However with relaxed muscles, the whole joint cross-section serves as an effective area for the internal pressure, and this area is reduced by muscle activity. At the same time, the effectiveness (with respect to movement of the metatarsus) of the flexors increases, since the antagonistic moment of the pressure is reduced. This mechanism is especially important if the pressure is induced by the activity of the flexors themselves. The Fl. met. bil. is therefore most suitable for quick and powerful flexions, while the Fl. met. long. and the Fl. met. acc. do not influence the moment of extension. They may instead serve to establish a resting position.

Articular membrane. By raising the hemolymph pressure, the articular membrane is inflated. If the membrane were mechanically isotropic, the axial tensions, developed at the edge of the tibia and the metatarsus (Fig. 12), would produce a torque opposing extension, proportional to both the pressure and the angle of rotation. At $\alpha = 180°$, the torques induced by stretching the membrane of the tibia-metatarsus joint would be opposite and equal to the torques developed by the hemolymph pressure directly.

By means of the bellows-like folding of the joint membrane, stresses are resolved radially, beneath the joint axis at the edge of the tibia. Thus opposing torques are avoided by reducing the axial stress components in the joint membrane. The enlarged radial forces are of the same magnitude as the joint forces and contribute to the deformation of the cuticle in the region of the tibia metatarsus joint.

Forces in static equilibrium. The deformation of the cuticle in the region of the slit sense organs largely depends on the magnitude and direction of the joint force. During static equilibrium, this

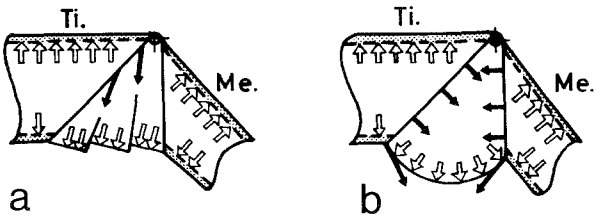

Fig. 12a, b. Mechanical design of the articular membrane. **a** The articular membrane of the tibia-metatarsus (*Ti, Me*) joint is folded like a bellows. In that way, axial tensions, developed in the membrane under pressure load, are resolved in tangential stresses applying at the dorsal edge of the tibia (⧫). **b** An unfolded isotropic membrane would lead to high torques (⧫) preventing extension

can be calculated from external and internal forces accessible by measurement.

The loads at the tibia-metatarsus joint are determined by the following *parameters:* (a) Hemolymph pressure, P, the moment $\vec{M}_P$ (comp. Eq. 6) and the tension ($\vec{M}_{\text{mem}}$) induced in the articular membrane. (b) The forces developed by the flexor muscles $\vec{F}_{\text{m}}$ (Fl. met. bil. und Fl. met. long) and the moments $\vec{M}_{\text{m}}$ they induce (comp. Eq. 5). (c) The ground reaction force $\vec{F}_A$ and the induced moment $\vec{M}_A$. (d) The tibia metatarsus angle, α.

The following parameters were found to be negligible: (a) Inertial forces (at walking speeds up to 10 cm/s, in bird spiders). (b) The masses of the tarsus (ca. 25 mg) and metatarsus (ca. 40 mg). (c) Torsion around the large axis of the metatarsus (low if the leg's surface of contact with the ground is small or if the friction of the surface is low, e.g. the substrate is sandy). (d) Torques, perpendicular to the main plane of measurement, developed by the Fl. met. bil, whose site of attachment is at the lateral metatarsus edge. During synergistic activity (comp. Seyfarth 1978a), no lateral moment could result about the middle condyle. (e) Forces and torques developed by the *Depressor ungium,* because it is small in cross section and has a short lever. However, due to its attachment in the joint region, it may influence the deformation at the site of the slit sense organs considerably. Its contribution to the joint force can be calculated following the procedure used for the flexor muscles.

The ground reaction force can be resolved into an axial (z′), lateral (y′), and dorsoventral (x′) component in a local system of co-ordinates that are fixed with respect to the metatarsus (comp. Chapter IV). In the following section, the *joint forces* induced by these component forces are described.

a) Axial force (Fz'), parallel to the long axis of the metatarsus: This force component induces an identical force vector at the tibia-metatarsus joint (Fig. 13). Torques are not developed.

b) Lateral force (Fy'), perpendicular to the long metatarsal axis and perpendicular to the main plane of movement. Moments and joint forces are

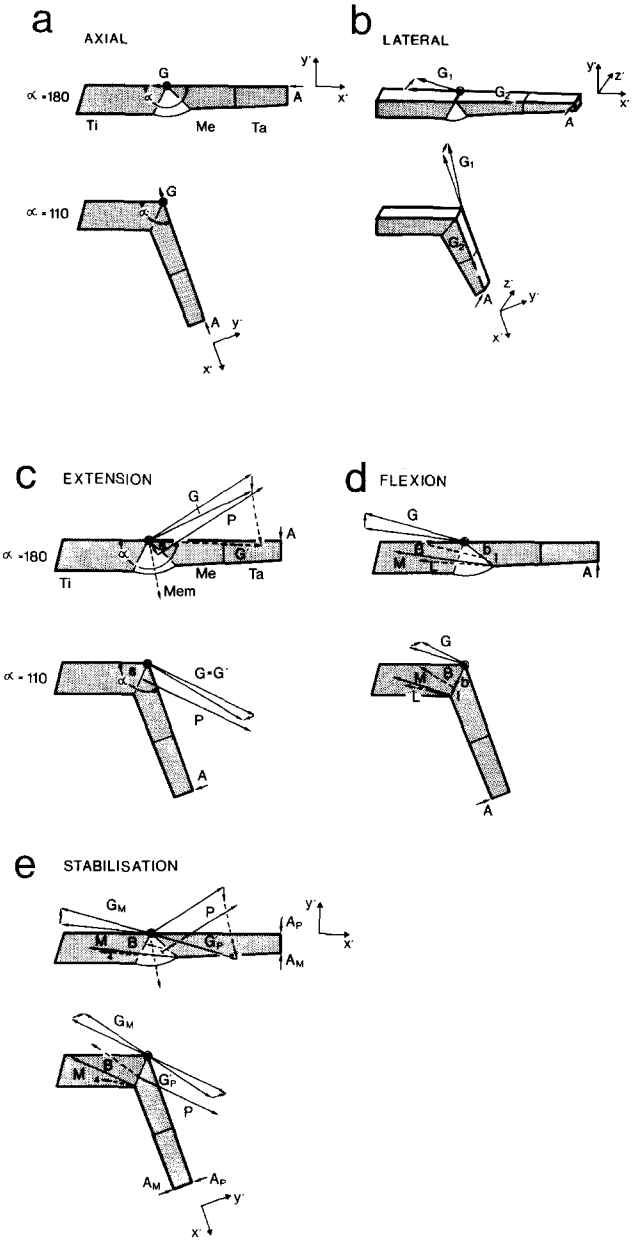

Fig. 13a–e. Calculated joint forces, developed by passive and active compensation of load. **a** Axial load (z'). The joint force (G) is similar to the force applied (A). **b** Lateral load (y'). The joint forces are directed almost parallel to the metatarsus with opposite sign anterior (G_1) and posterior (G_2) and amount ca. fourfold the load applied (A). **c** Extension (dorsoventral load, x'). The joint force (G) is the sum of applied force (A), and the force developed by the pressure (P) at the centre of gravity of the effective area. If the membrane forces (*Mem*) are added the force G' results. The direction of G' changes only by about 20° if the metatarsus is rotated by 70° ($\alpha = 110°$) and it amounts to less than fourfold of the force applied. **d** Flexion (dorsoventral load, x'). The joint force $G = G'$ is equal to the sum of the applied force (A) and the muscle force (M) which in turn results from the sum of the forces developed by the *Fl.met.long.* (L, l attachment of the tendon) and the *Fl.met.bil.* (B, b centre of the surface of attachment). The direction of G' changes by about 10° by rotating the metatarsus through 70° ($\alpha = 110°$) and it accounts for four- to eightfold the force applied (A).

determined by levers, i.e. limb and joint geometry. The forces induced at the anterior and posterior condyle of the joint act in opposite directions and are almost parallel to the metatarsus which, in tarantulas, can reach more than four times the lateral component of the ground reaction force.

c) Dorsoventral force (Fx'), perpendicular to the long axis of the metatarsus and in the main plane of movement: This component of the ground reaction force is determined by internal forces (Fig. 10). If the muscles compensate for the ground reaction force as in tarantulas, the joint force taken as a function of α is about four to eight times the dorsoventral force component. The direction of the joint force, depending on that of muscle fibres, only varies by about 10°. Joint forces can reach values up to eight times that of the ground reaction force, if it is compensated for by hemolymph pressure. The direction of the joint force changes, in proportion to α, by about 90°. If the membrane force is added, this change in direction is reduced to about 20°. The joint forces developed by both muscles and hemolymph pressure are similar in magnitude but opposing in direction (160°–180°). If the various muscle forces are assumed to be different and are dependent on α, resulting zero torque and zero joint force can be brought about for every tibia-metatarsus angle. Thus it is possible to stabilize the joint position by internal forces, without any consequential joint load. As a result, in slow locomotion the joint forces during the return stroke are low due to the compensating effect of muscle forces and hemolymph pressure. In contrast, during the power stroke they are higher than 120 mN, and induced by muscle forces compensating for a dorsoventral component of the ground reaction force of ca. 40 mN (see Chapter IV).

2.3 Strains in the tibia

Strain magnitude. The skeleton of the tibia is a thin-walled cuticular tube (diameter: 4 mm; wall-thickness: 35 µm; Young's Modulus: 18 kPa). For this tube the maximal strain/force-ratios (s/F) can be predicted for axial, lateral and dorsoventral loads applied at the tarsus tip (length of tarsus and metatarsus: 17 mm; see Szabo 1972, 1975):

e During stabilization of a certain joint angle by the antagonistic muscle forces and hemolymph pressure, their moment is compensated ($A_P = -A_M$) and the resultant joint force ($G'_P + G_M$) diminishes. Even situations with zero joint force are possible (extended leg: higher activity of the Fl.met.long.; flexed leg: higher activity of the Fl.met.bil.)

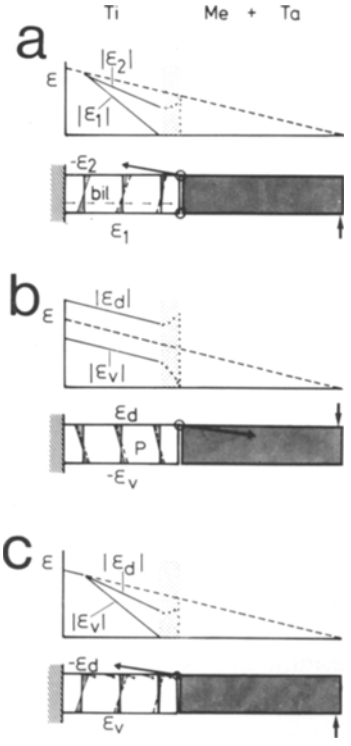

Fig. 14a–c. Schematic drawing of strains in the tibia during bending load including the expected influences of distributed muscle attachments and of hemolymph pressure. Above: strain distribution (———) in the tibia (--- distribution in a tube for comparison; ▨ joint region); below: load condition (tibia clamped at its proximal end; force applied at the leg's tip; ε strain, *v* ventral, *d* dorsal). **a** Bending load during lateral deflection (dorsal view; $\alpha = 180°$). The articular membrane can be unloaded by the activity of the Fl.met.*bil.* (→ → →). Thus the bending load of the joint region is reduced. **b** Extension (lateral view). The negative strains induced by bending are lowered by internal pressure. If hydraulic extension is assumed for the patella-tibia joint too, only low bending moments act on the skeleton of the tibia. **c** Flexion (lateral view). The distribution of the muscle attachment (Fl.met.bil. ↘ ↘ ↘) leads to a reduction of the bending moments distally. If the patella muscles and the Fl.met.long. are taken into consideration even the proximal bending moments are diminished

a) Axial load (z'; proximal end of tube fixed): $s/F = 0.126$ με/mN (parallel to the tibia axis).

b) Bending load (y', x'; proximal end of tube fixed): $s/F = 3.5$ με/mN (near the clamped proximal end, parallel to the long tibial axis).

c) Hemolymph pressure (x', extension; effective area: tube cross section; bending load neglected): $s/F = 2.1$ με/mN (perpendicular to the tibia axis, parallel to the long tibial axis: $s/F = 1.0$ με/mN).

d) Torsion (y'; tube end fixed): $s/F = 1.0$ με/mN (45° to the long tibial axis, bending neglected).

It follows that, in a tube resembling the tarantula's tibia, the maximum positive strain (dilatation) of ca. 5.5 με/mN can be developed by extension of the metatarsus (hemolymph pressure and bending) and the maximum negative strain (compression) by lateral bending of the straightened leg. The calculated values agree well with the strain values measured at the distal end of the tibia (see Chapter III).

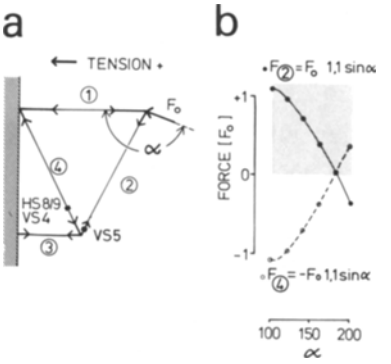

Fig. 15a, b. Simple mechanical model, which explains the dependence of the strains measured at site of the slit sense organs on the angle of the joint force. **a** Frame work. Bar ④ is oriented perpendicular to the long slit axis of the lyriform organs *HS8*, *HS9*, and *VS4* (■); bar ②, at the edge of the tibia, perpendicular to the organ *VS5* (■). **b** the dependence of the strains in these organs on α presumably corresponds to the dependence of forces, *F*, in the bars ($\sim \sin\alpha$)

A precise prediction of strain requires elaborate mathematical calculations or experiments considering the true shape of the tibia and natural load conditions. Photoelastic models are currently being investigated. However, the qualitative influence of some structural details are easily seen (Fig. 14):

a) A thickening of the cuticle near the condyles and at the attachment of the Fl.met.long. lowers the strains. The attachment of the Fl.met.bil. is not thickened.

b) A thickening of the proximal and distal edges of the tibia increases the torsional stiffness of the obliquely cut tube (Szabo 1972).

c) The tension in the articular membrane connecting the segments can be lowered, under lateral load ($\alpha = 180°$), by the activity of the flexor muscles.

d) During extension, hemolymph pressure lowers negative strains.

e) Flexor muscles in the tibia accept bending loads and lead to an increase of normal stresses. Taking the muscles in the patella into account, which attach at the proximal end of the tibia, bending moments can be largely reduced in the tibia under natural conditions.

Compression of the slit sense organs under various loads. The simplest model to interpret load conditions that lead to a compression of the organs is a framework (Fig. 15). Two rods are oriented per-

pendicularly to the long axes of the slit sense organs HS8, HS9, VS4 and VS5. The forces in these rods can be taken to be proportional to the developed strains (s_i) at the sites of the slit sense organs and depend on the sign and direction (α) of the joint force (F_0). With respect to the different components of load applied to the tip of the metatarsus and the tibia-metatarsus angle, compression of the organs is expected in the following situations:

Axial pressure load (x'). Joint force: Identical with the force applied. Prediction: Compression of the organs *HS8, HS9* and *VS4* for $90° < \alpha < 180°$, dilatation above 180° (see Eq. 9).

$$\text{strain} \sim \text{Force} \cdot \sin\alpha. \tag{9}$$

Inverse dependence at the organ *VS5*; compression above 180°.

Lateral load (y'). Joint force: Direction strongly depends on α similar to axial load. Prediction: Compression of the organs *HS8, HS9,* (*VS4*) for $90° < \alpha < 180°$ during posterior (anterior) deflection and for $\alpha < 180°$ during anterior (posterior) deflection. The sector of joint angles where compression is expected may deviate, because the deformation of the distal tibia is not exactly symmetrical anteriorly and posteriorly (Blickhan, in prep.).

Dorsoventral load (x'). Joint force: Direction almost independent of α. Prediction: For the organs *HS8, HS9* and *VS4* compression is induced by muscle forces and for the organ VS5 by hemolymph pressure.

All predictions agree well with direct measurements (see Chapter III) and with electrophysiological experiments and studies on plastic models (ref. Barth 1981), as far as similar situations were investigated.

3 Discussion

3.1 Design of skeleton and joints

The peripheral arrangement of cuticle in the spider leg results in high bending stiffness (Galilei 1638; Wainwright 1969; Darnhofer-Demar 1977). However, the *thin walled tibia* can easily fail by buckling (Szabo 1972). This weakness is compensated for by the internal pressure (Currey 1967). Even if buckling did occur, for example, by an unexpected impact, the leg can be inflated, straightened and stabilized by an increase in hemolymph pressure. As long as the surrounding structures are able to accept tension stress, pressure loads can be absorbed by the internal lymph. The torque of 0.5 Nmm sufficient for buckling of the tibia in the region of the tibia metatarsus joint (Blickhan, in prep.) can be compensated for by a hemolymph pressure of ca. 20 kPa, (maximum pressure: ca. 100 kPa). An unloaded leg can be straightened with the aid of lower pressures and even torques induced during slow locomotion (<1 Nmm) can be accepted.

By contrast, in the legs of vertebrates, pressure loads can only be taken up by the skeleton (Pauwels 1949/50; Nachtigall 1977).

During ecdysis, the hemolymph pressure may be the main structural element in spiders absorbing pressure loads. The still flexible cuticle is probably tension loaded, but as yet, there is no experimental evidence for a hydraulic skeleton during that period (Wainwright 1969; Chapman 1975).

Support of loads by means of internal pressure not only reduces stresses at the condyles and thus allows a reduction of the condylar surfaces, but also simplifies joint construction. Without hemolymph pressure cuticular load bearing structures are necessary, and determine the axis of rotation.

3.2 Hydraulic movements of appendages

The development of torques by means of internal pressure should be possible in many joints in the skeleton of arthropods.

Insects. During hatching, pupation and imaginal ecdysis a high hemolymph pressure (>10 kPa) serves as an antagonising agent to muscles (Chapman 1958) and enables insects to make hatching and fossorial movements (Cortrell 1962; Zdarek et al. 1979; Elliot 1981). But even lower pressure values (<2 kPa), for example, those that occur in adult locusts (Bayer 1968) can be sufficient to move appendages. Respective measurements on dragonfly larvae (Tanaka and Hisada 1980) can be easily interpreted by applying Eqs. 6 or 7.

Crustaceans. Hydraulic movement of the limbs of crustaceans can not be ruled out despite the fact that pressures measured so far have been quite low (<3 kPa; Picken 1936; Burger and Smythe 1953). During underwater locomotion, even small torques can produce slow movements, because weight is reduced to 11% of its original value by buoyancy. A direct indication of hydraulic action is provided by the eye stylus eversion of *Carcinus* (Alexander 1979).

Chelicerata. Considering Eqs. 6 and 7, the development of torques by internal pressure in spiders is possible not only in the tibia-metatarsus and fe-

mur-patella joint as has been emphasised in the literature (Parry and Brown 1958b), but in every leg joint.

At the metatarsus-tarsus joint of spiders, where all necessary anatomical data were measured, the application of Eq. 6 allows an explanation of the joint kinematics (Speck and Barth 1982).

3.3 Expected strains and functions of the slit sense organs

According to simple mechanical models, in the spider's tibia maximum strain is generated in its proximal end by bending load. However, direct measurements have demonstrated that failure of the tibia under a load applied laterally at the tip of the metatarsus occurred in the distal joint region (Blickhan, in prep.). Taking into account that bending and strain especially at the tibia's distal end can be reduced by muscles accepting tension load, strains induced by lateral load applied to a flexed leg (torsion of the tibia) may be most dangerous. The latter situation is expected to lead to a maximum compression of the lyriform organs at the tibia-metatarsus joint. This result is consistent with earlier studies (Barth and Bohnenberger 1978) and verified by strain measurements (see Chapter III). The strain at the site of organ HS8 can be lowered by straightening the leg under load and thus reducing torsion.

On the other hand, the campaniform sensilla at the proximal tibia of the cockroach (Zill and Moran 1981a, b) showed maximum response to dorsoventral bending of the tibia. One must take into consideration that the tibial torsion, induced by lateral load in the distal leg segments of this animal is low, because the distally adjacent segments are short and coupled by compliant joints. Therefore, bending induces the highest strain in the tibia of the cockroach under natural load.

For the spider and the cockroach, the load of the tibia most sensitively registered by the organs may be, with respect to this leg segment, the most dangerous one that occurs under natural conditions.

III. Strains developed by external and internal forces

Different slit sense organs may be specialized to measure particular loads due to their specific position in the exoskeleton. The presence of such spezializations could also lead to differences in mechanical sensitivity, defined as the inverse ratio of the applied load to induced strain. To date, the sensitivity of these slit organs has only been investigated in the organ HS8 under a single load condition using electrophysiological methods (lateral load, $\alpha = 130°$; Barth and Bohnenberger 1978; Bohnenberger 1981).

With the methods described above (Chapter I) strain in the spider cuticle could be measured for the first time as a function of load. Due to the dorsal arrangement of the rotational axis of the tibia-metatarsus joint, muscle forces and hemolymph pressure are antagonists and thus could easily be separated (see Chapter II). The load conditions, chosen in the present study, were adapted to the degrees of freedom of the joint (Blickhan, in prep.). By dividing the ground reaction force into components corresponding to these load conditions, and adding the strain components measured for each force component in the tethered animal, strains occurring in the tibia of freely moving spiders could be predicted (see Chapter IV).

1 Material and methods

Experimental arrangement. The animals were tethered with adhesive tape to a brass dummy and the leg to be investigated (leg 2) was fixed by dental cement casting (Fixodont, De Trey) in the region of the patella-tibia joint (Fig. 16). The metatarsus was deflected (up to 1 mm ≙ 3.5°) by a feedback controlled (comp. Bohnenberger 1981) electrodynamic vibrator (V 106, Ling). The forces, induced at the site of deflection at a distance of 16 mm from the tibia-metatarsus joint, were measured by the force transducer described above. The input deflection functions were triangular, sinusoidal and trapezoidal. Due to varia-

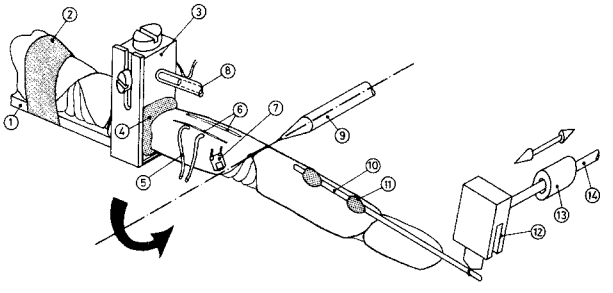

Fig. 16. Experimental arrangement. The animals were tethered with adhesive tape (*2*) on a brass dummy (*1*). The investigated leg was fixed between the dummy and the pressure transducer (*3, 8* reference channel) at the proximal end of the tibia by casting in dental cement (*4*). The position of the animal was adjusted to allow its rotation about the axis of the tibia-metatarsus joint (*9* spine in the axis of rotation). A steel needle (*10*) glued with fast setting cement (*11*) onto the metatarsus was attached to a force transducer (*12*) which was moved by an electrodynamical vibrator (*13* displacement transducer; *14* axis of the vibrator). Strains induced in the tibia were measured by strain gauges (*7*). At the site of attachment of the Fl.met.bil. (*6*) electrodes for muscle stimulation and the registration of myograms were implanted (*5*)

tions in leg geometry of different individuals, the adjustment of a corresponding tibia-metatarsus angle (straightened leg: $\alpha = 180°$) was limited to within $\pm 10°$.

Torques actively developed in animals stimulated by brush strokes could be assigned to muscle forces or hemolymph pressure with the aid of pressure measurements and myograms. In addition, electrical stimulation of the muscles and pressure application via the reference channel of a pressure transducer allowed the contribution of these antagonistic parameters to be measured independently.

To reduce the influence of external vibrations the mechanical set-up was mounted on a weighing table, which was separated from the surrounding Faraday cage. The simultaneously measured data (deflection, angle, force, strain, hemolymph pressure, muscle-potentials, muscle-stimulation, temperature and the trigger signal) were stored on fm-tape and processed using a laboratory computer (Med 80, Nicolet).

Data evaluation. Strain, force, deflection, and pressure signals were averaged over 10 periods to improve the signal-noise ratio. The first five signal periods were discarded, because in some cases higher force amplitudes were measured initially. The true deflection of the metatarsus was calculated by subtracting the deflection of the loaded force transducer from the displacement obtained at the axis of the vibrator.

Strains at the organs, generated by forces applied to the metatarsus tip, can be described by single strain-force ratios, called mechanical sensitivities, because the strain-force characteristics are linear. However, due to the non-linear joint stiffness (Blickhan, in prep.) this does not hold for the dependence of strain on deflection of the metatarsus. Under internal loading, mechanical sensitivity was defined as the ratio of the maximum strain and force values reached during a single peak when the animal was stimulated. The same torque can be produced by different distributions of muscle forces and hemolymph pressure. Thus the corresponding joint forces and the strain induced at the organs' site are not determined equivocally.

2 Results

Strains, induced by forces applied to the metatarsus tip, were measured at lyriform organs HS8, HS9, VS4 and VS5, near the tibia-metatarsus joint and by the attachment site of the Flex.met.bil. on the dorsal tibia (TiOl, TiOq; see Chapter II).

2.1 *Axial load – z'*

Under axial load (parallel to the metatarsus), the mechanical sensitivities of the lyriform organs described in detail below are in the range of ± 8 $\mu\varepsilon$/mN (Fig. 17).

HS8, HS9 at the posterior and *VS4* at the anterior tibia: These organs can be considered to have similar positions with respect to their axial loading (see Chapter II), and hence there is also a similarity in the way their sensitivities depend on the tibia-metatarsus angle. Compression, the adequate stimulus, occurs under pressure load when $\alpha < 170°$, and under tension load when $\alpha > 170°$. The organs are insensitive to axial load at an angle of $170° \pm 10$ SD.

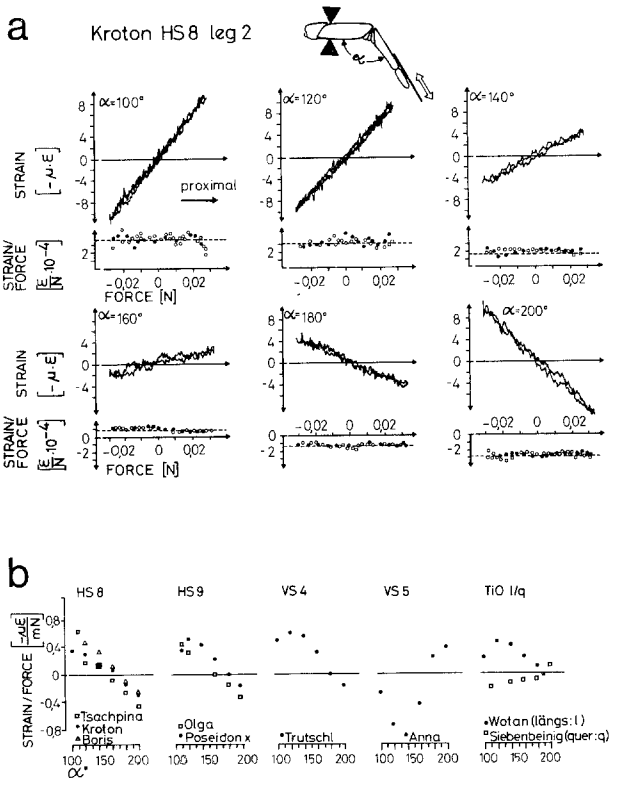

Fig. 17a, b. Strain at the tibia during loading parallel to the long metatarsal axis (axial, *z'*). **a** Strain at organ *HS8* as a function of the force applied at the metatarsus tip (arrow) and its dependence on the tibia-metatarsus angle α. The strain force characteristics are linear and free of hysteresis. The mechanical sensitivity (strain/force) is defined by the slope of the characteristics (force direction: ● proximal, ○ distal). It is independent of the amount of load but changes with α. **b** Mechanical sensitivities (*strain/force*) as a function of the tibia-metatarsus angle α for different slit sense organs near the tibia-metatarsus joint (*HS8, HS9, VS4* and *VS5;* □ ● △ different animals) and at the dorsal tibia (*TiOl/q*; l parallel, q at a right angle to the long tibial axis). For the slit sense organs HS8, HS9, and VS4 the dependence on α is similar. In the region of the organ VS5 the sensitivities are opposite for $\alpha < 110°$

VS5, at the ventral tibia: When $\alpha > 120°$, the ratios are nearly the reverse of those measured for the organs above. This organ is compressed under tension load if $\alpha < 180°$, and under pressure if $\alpha > 180°$.

Measurements taken at the site of muscle attachment on the dorsal tibia (*TiO*) show that the strains induced are low. In this case also, the sign changes at ca. 185°. In the directions parallel and perpendicular to the long tibial axis the dependence of the strain-force ratio on α is opposite. Under pressure load the cuticle is compressed parallel to this axis.

In all cases sensitivities under axial load are low when the leg is extended. In some measurements, a sinusoidal dependence of the sensitivity

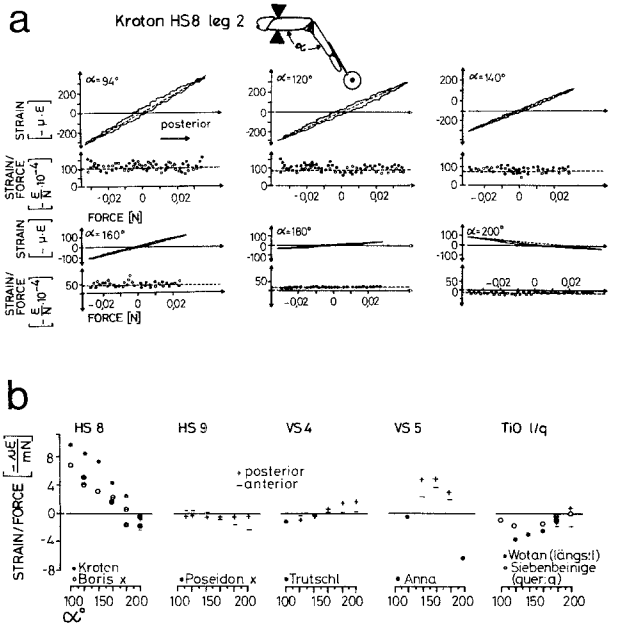

Fig. 18a, b. Strain at the tibia during lateral loading (y') of the metatarsus. **a** Strain at organ HS8 as a function of the applied force (◉ arrow perpendicular to the image plane) and its dependence on the tibia-metatarsus angle α. The characteristics are linear and change their slopes with α (force direction: • posterior, o anterior). **b** Mechanical sensitivity for the slit sense organs *HS8, HS9, VS4,* and *VS5,* respectively, and the dorsal tibia (*TiO*l/q; l parallel to long axis, q at right angle to it) as a function of the tibia-metatarsus angle α. (Scales in Figs. 17b and 18b differ!) The dependence of the sensitivity on α is similar to that found during axial loading of the HS8 organ. The sensitivities of the organs HS9 and VS4 are roughly opposite (force direction: + posterior, −anterior)

on α could be observed (see Chapter II). The inter-individual variability is caused by the uncertainty in the reference angle ($\alpha = 180°$). The angle, at which the sensitivities are zero, ($\alpha = 172°$) varies by $\pm 10°$ SD.

2.2 *Lateral load – y'*

Starting from the resting position ($\beta = 0°$), the sensitivities during anterior and posterior deflection (Fig. 18) are quite different in some cases. The sensitivity range is more than ten times that under axial load, with a maximum of ca. 10 με/mN. The strain-deflection ratio is rate as well as deflection dependent, with a maximum of 1000 με/mm (≙286 με/degree). Compared to the values found with axial load, this is lower by a factor of 0.2.

HS8, at the posterior tibia: When under lateral load, the dependence of the sensitivities on the tibia-metatarsus angle, α, resembles that found under axial load. The organ is compressed by posterior deflections if $\alpha < 180°$, and by anterior deflections if $\alpha > 180°$. Again, at $\alpha = 180°$, the organ is insensitive to lateral load.

HS9, dorsal to organ HS8: For anterior and posterior deflection, the strain-force characteristic has different gradients and the organ's mechanical sensitivity is lower than that of the organ HS8: During posterior deflection, it is lower than 1 με/mN and almost independent of α, while during anterior deflection it reaches up to 3 με/mN and changes the sign at ca. 150°. Accordingly, a compression of the organ is induced by anterior deflection if $\alpha > 150°$.

VS4, at the anterior tibia: The dependence of the sensitivity on α is approximately opposite to that measured at organ HS9. During anterior deflection it is low (< 0.5 με/mN; $120° < \alpha < 200°$), and it reaches 2 με/mN during posterior deflection. The organ is compressed during posterior deflection if $\alpha > 150°$.

VS5 at the ventral tibia: This organ is compressed between 120° and 190° during anterior loading. For large and small angles, the region of the dorsal and ventral limits, strains are induced by stress in the joint membrane.

Negative strains are developed by anterior deflections of the metatarsus at the dorsal tibia (*TiO*) perpendicular to the long tibial axis at the site of the posterior muscle attachment, and parallel to the long tibial axis at the site of the anterior muscle attachment.

2.3 *Dorsoventral load – x'*

In freely running animals, moments generated by the dorsoventral component of the ground reaction force are actively compensated for by internal forces (see Chapter II). Consequently the mechanical sensitivity of the slit sense organs during dorsoventral load was estimated during active development of torques by muscle forces and the antagonistic hemolymph pressure (Fig. 19).

HS8, at the posterior tibia: The mechanical sensitivity of this organ, with respect to moments induced by internal forces, amounts to 2.5 με/mN ± SD and is independent of α. The strain is proportional to the developed moment and thus to the joint force also. Compression is induced by muscle activity.

HS9, dorsal to organ HS8: Here the mechanical sensitivities ($\alpha = 150°$) during extension (6.9 με/mN ± 1.2 SD) and flexion (1.35 με/mN ± 0.7 SD) are different ($P < 0.001$). Like the organ HS8 this organ is compressed by muscle load.

VS4, at the anterior tibia: Again, this organ is more sensitive to extension by hemolymph pres-

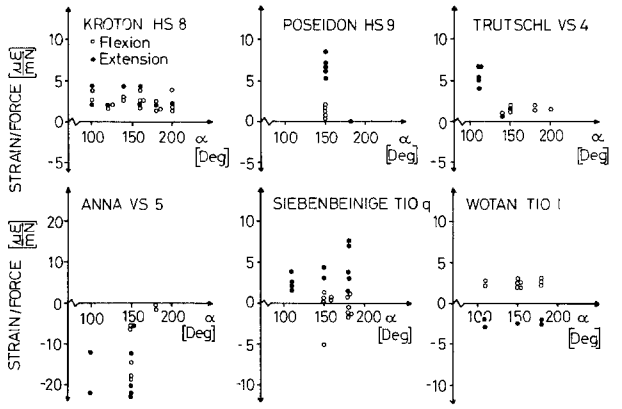

Fig. 19. Mechanical sensitivities (*strain/force*) of the slit sense organs *HS8, HS9, VS4,* and *VS5* and that found on the dorsal tibia (*TiOl/q,* see Fig. 18) during active, dorsoventral load (x'; • extension, o deflection). The organ HS8 has the same sensitivity during extension and flexion, independent of α. All other organs are more sensitive to extension than to flexion. At the dorsal tibia, parallel to its long axis, flexion as well as extension leads to compression of the cuticle

sure (5.6 με/mN ± 1.4 SD; $\alpha = 100°$) than to flexion by muscle forces (1.4 με/mN ± 1.4 SD), and compression occurs under muscle load. The sensitivities of the organs VS4 and HS9 are very similar.

VS5 at the ventral tibia: At this organ, a rise in hemolymph pressure produces compression, while muscle forces cause dilatations. Again, the sensitivities for both extensions (−16.4 με/mN ± 6.8 SD) and flexions (−8.0 με/mN ± 6.8 SD) differ ($P < 0.05$). The reason for the relatively high sensitivities was a repaired fissure in the ventral tibia, resulting in a lower joint stiffness. The values, normalised to correct the stiffness (mean: −4.7 με/mN ± 2.1 SD; extension: −5.0 με/mN ± 2.1 SD; flexion: −2.5 με/mN ± 2.1 SD) are similar to those, measured at the other adjacent slit sense organs.

At the dorsal tibia, perpendicular to its long axis (*TiOq*), the sensitivities display different signs. As one might expect, the skeleton tube is dilated by hemolymph pressure (2.9 με/mN ± 1.5 SD). During flexion, both positive and negative strains were measured (0.4 με/mN ± 1.5 SD). The negative strains can be attributed to muscles, attaching distally to the measurement point.

Parallel to the long tibial axis (*TiOl*), negative strains are measured during both flexion (2.0 με/mN ± 0.4 SD) and extension (−1.8 με/mN ± 0.4 SD).

2.4 Contribution of the active parameters

As far as active parameter contribution is concerned, only peak values were considered in the previous section. If one considers the time courses of the different parameters, then further statements about mechanical relationships are possible.

Stimulation with a brush. To elicit natural responses the animal was stimulated by touching its abdomen with a brush. The force-time relationships taken from the metatarsus tip and those from simultaneously measured strains are very similar, whilst the time course of the hemolymph pressure is clearly different (Fig. 20). The changes in pressure are slower than those for force. The electrical myograms have substantiated the activity of the Fl.met.bil. during steep rises in the force.

Muscle stimulation. The sensitivities measured during electrical stimulation of the Fl.met.bil. are similar to measurements taken from animals stimulated by a brush. The moment of extension succeeds the pressure pulse without delay and the delay between stimulus and measurable force amounts to approximately 30 ms (Fig. 21 a).

Applied pressure. In experiments where the pressure in the dorsal hemolymph channel was raised artificially using the reference channel of the pressure transducer, the brush measurements were again confirmed. For example, the negative strain measured parallel to the dorsal muscle attachment during extension could also be induced by hemolymph pressure. In most cases, the maximum moments lag considerably behind the applied pressure, however, this is not found during pressure pulses developed by the animal (Fig. 21 b).

Taking evidence from adjustable flow resistances (see Chapter II) it can be seen that not every pressure pulse generated in the proximal leg is transmitted distally. This is consistent with the observation that a large volume of Ringer's solution can be pumped proximally into the animal, without any measureable moment of extension in the distal leg.

2.5 Time dependence of strain

In all measurements, the strain-time relationship closely resembles the force-time relationship. This corresponds to the linear strain-force characteristics and narrow hysteresis.

The relaxation of strain (s) during step deflection (power function: $s \sim t^{-k}$, lateral: $k = 0.09$, axial: $k = 0$; Fig. 22 a) is similar to that of the force, measured at the metatarsus tip (Blickhan, in prep). This is supported by the measured transfer characteristics (power function: $s \sim f^k$; $k = 0.06$; phase (φ) drift: $10° < \varphi < 20°$; Fig. 22 b), and thus viscoelastic properties of the strain gauge and the glue have

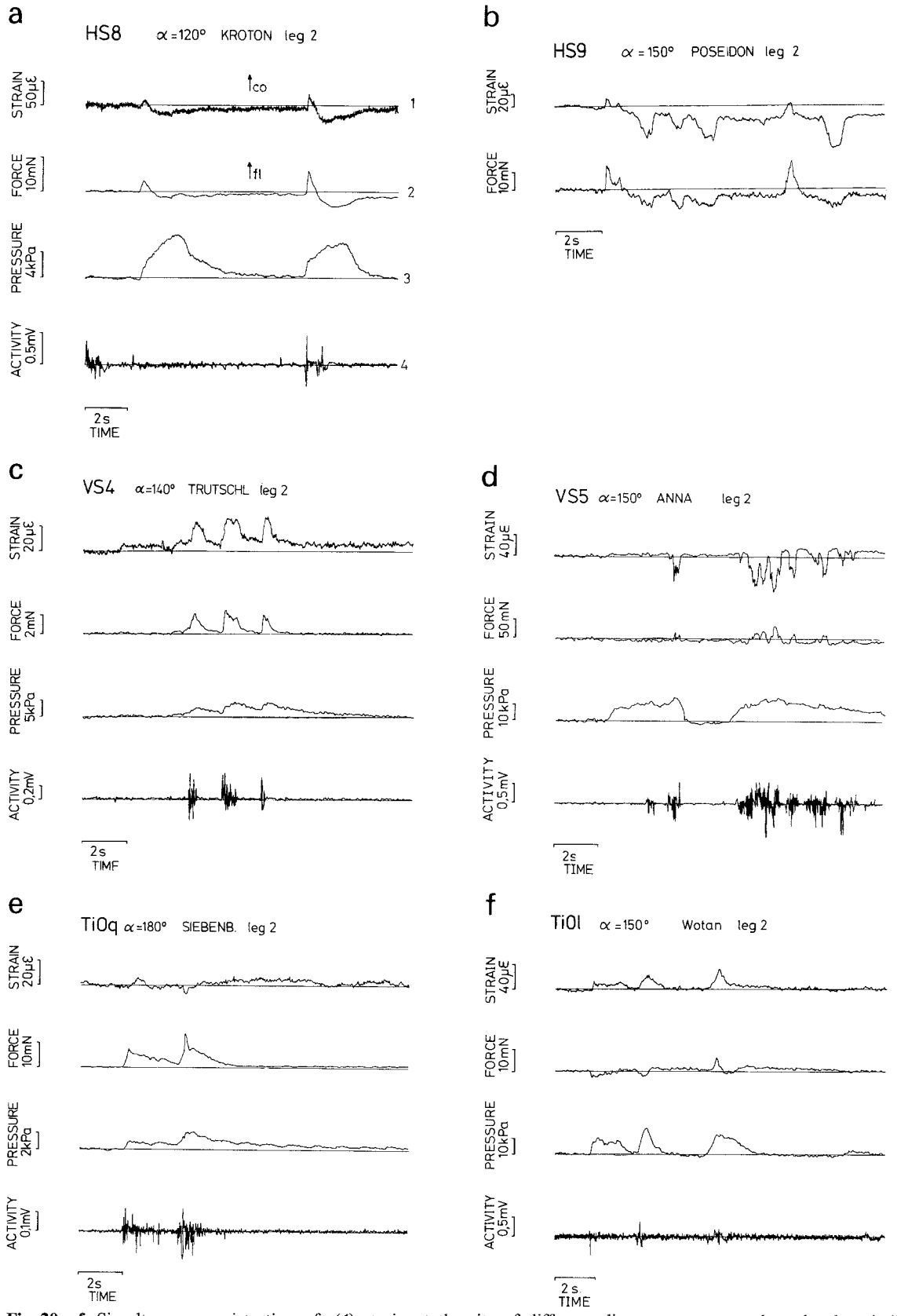

Fig. 20a–f. Simultaneous registration of: (*1*) strain at the site of different slit sense organs and at the dorsal tibia, (*2*) of the dorsoventral force component induced at the metatarsus, (*3*) of the pressure in the dorsal hemolymph channel, and (*4*) of the activity of the Fl.met.bil. In general the time courses of strain and force are very similar. **a** HS8: In a flexed leg ($\alpha = 120°$) besides of fast flexions, slow extensions occur which in turn lead to dilatation of the organ. **b** HS9, $\alpha = 150°$: Flexion induces compression and extension much higher dilatation. **c** VS4, $\alpha = 140°$: Activity of the flexors generates compression. **d** VS5, $\alpha = 150°$: Activity of the flexors induces dilatation, increase of pressure compression. **e** TiOq, $\alpha = 180°$: During flexion compression and dilatation can be measured at the site of attachment of the Fl.met.bil., at a right angle to the long tibial axis (*q*). **f** TiOl, $\alpha = 150°$: Parallel to the long tibial axis (*l*), extension and flexion induce compression

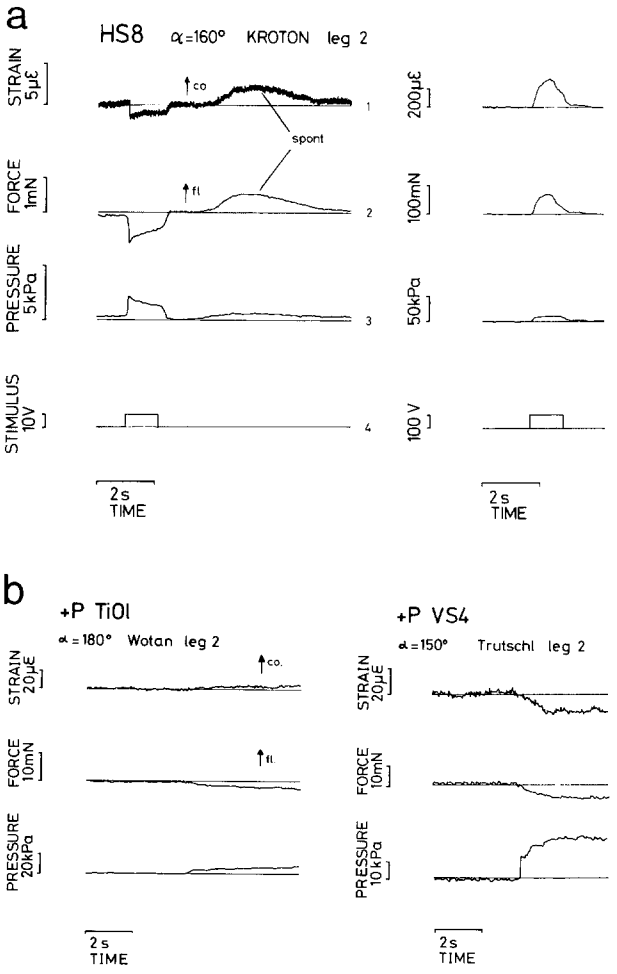

Fig. 21 a, b. Electrical muscle stimulation and external increase of hemolymph pressure. **a** Electrical stimulation of the Fl.met.bil. Left: Stimulation (*4*) with an applied voltage of 10 V induces extension (*2, fl* flexion). Pressure pulse (*3*), extension (*2*) and strain (*1, co* compression) at the organ HS8 become measurable after a delay of 30 ms. The following spontaneous (*spont*) flexion induces an increasing hemolymph pressure and a compression of the organ HS8. Right: Stimulation with an applied voltage of 110 V induces flexion during identical conditions. **b** By external increase of the pressure (+*P*) in the tibia, sensitivities similar to those measured during spontaneous extension were found. Left: at TiOl – The applied pressure induces extension (*fl* flexion) of the joint and compression of the cuticle (*co* compression) at the dorsal tibia. Right: at VS4. The applied pressure gradually increases extension and dilatation of the slit sense organ

been proven to be negligible up to 10 Hz. For higher frequencies, these can be extrapolated, as only stiffening is expected to occur.

3 Discussion

3.1 Slit sense organs as force receptors

Articular strain correlates highly with the force at the leg tip and slit sense organs perceive this force by measuring this strain.

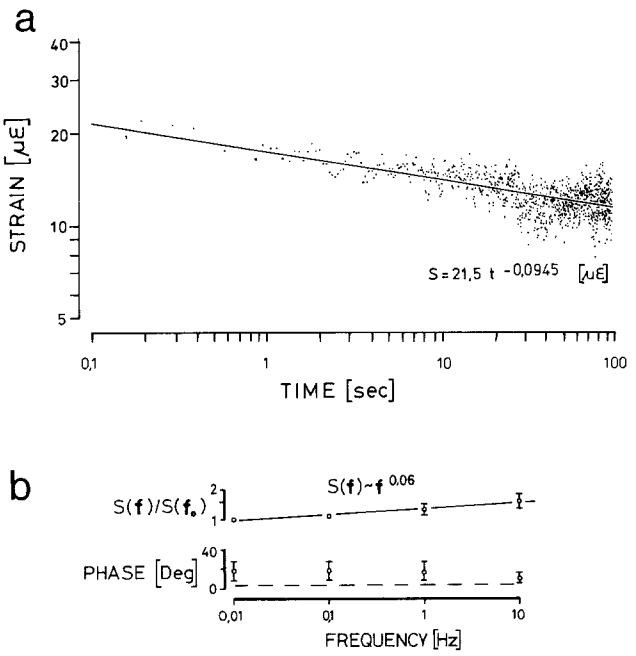

Fig. 22 a, b. Time dependence of strain. **a** The step response of the strain (*s*) measured at the site of the organ HS9 during lateral deflection is mainly determined by the joint stiffness and can be described using a power function. **b** Bode-plot of strain (*s*) for lateral deflection (70 µm) normalized to $s(f_0 = 0.01$ Hz). Sites of measurement: HS8, HS9, TiOq; $N=4$, $n=3$–100, ±SD

The nomenclature and classification of the receptors depends upon the level used for characterisation. At the level of the receptor, the slit sense organs measure the displacement of two points in the cuticle; the organs are 'displacement receptors' (Barth 1981). Regarding them as part of the whole exoskeletal structure they can be looked upon as 'strain receptors' (Barth 1978) which, like strain gauges, measure the local deformation of the skeleton. On a tertiary level the slit organs form points of a reference system including the whole leg. Here the organs are 'force receptors' (Seyfarth 1978b) sensing forces which induce skeletal deformation.

A nomenclature, using the whole animal as a reference system, should include information on which type of physical input is used by the animal. This input may be the deformation of the skeleton (e.g. to avoid destruction), or perhaps the animal could perceive through these deformations the forces applied to the skeleton. The term, 'displacement receptor' is not very suggestive in this case, since the desired piece of information is surely not just the displacement of the slit edges.

3.2 Specialization of the organs to specific loads

The present study confirms the hypothesis that certain slit sense organs, because of their position and orientation in the skeleton alone, are specialized for the measurement of specific loading parameters. However, a very narrow specialization to a

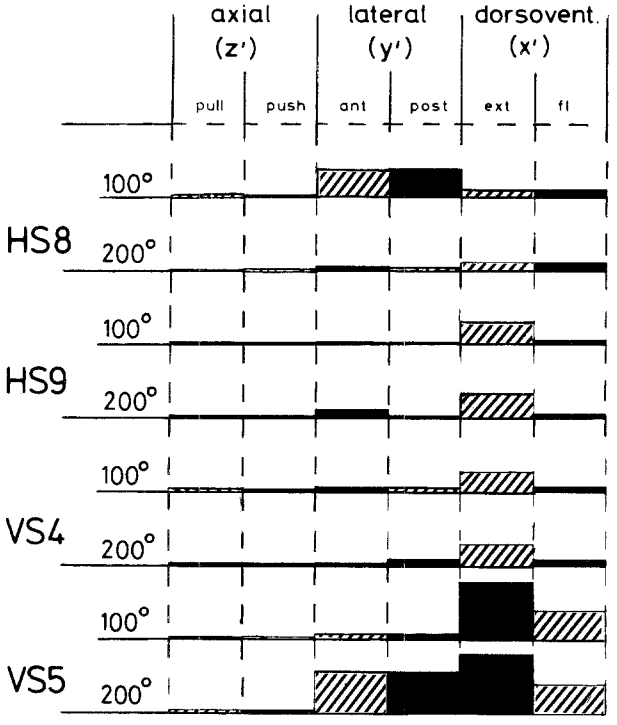

Fig. 23. Compression (adequate stimulus, black) and dilatation (hatched) of the lyriform organs HS8, HS9, VS4 and VS5 during different loads applied to the metatarsus: axial z' (pull and push), lateral y' (anterior and posterior) and dorsoventral x' (flexion and extension) Metatarsus flexed $\alpha = 100°$, extended $\alpha = 200°$

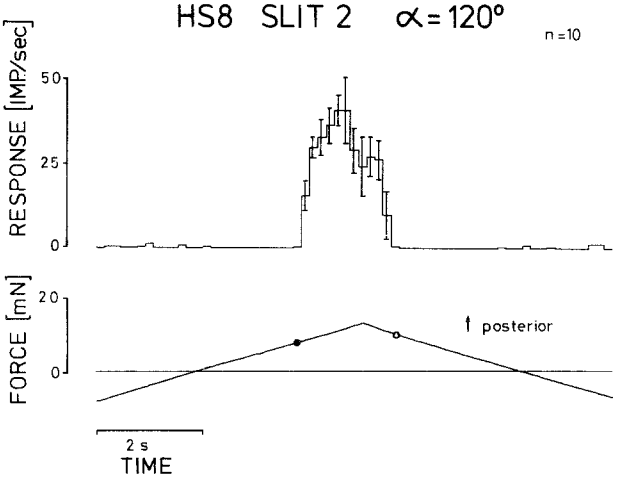

Fig. 24. Receptor response (post stimulus time histogram, ±SD) of the second slit of the organ HS8 of a theraphosid during lateral deflection of the metatarsus (length 17 mm). Threshold during posterior loading amounts to 8 mN (●) and during unloading to 10 mN (○). A force of 10 mN (deflection: 85 nm ≙ 0.28°) induces a strain of 60 με at the site of the organ HS8

certain load, (e.g. lateral load, $\alpha = 150°$,) was not found in any slit sense organ measured (Fig. 23).

3.3 Mechanical sensitivity and mechanical models

The extent to which the direct measurements of the strains in the region of the organs agree with predictions based on simple mechanical models described in Chapter II is discussed below.

Strain amplitude. The magnitude of the strains predicted for a cylindrical tube, similar to the spider's tibia, roughly agree with the measured values (axial load: < 0.8 με/mN, prediction: 0.1 με/mN; lateral load: 10 με/mN, prediction: 2.5 με/mN; dorsoventral load: < 10 με/mN, prediction: 3 με/mN). There are differences of up to a factor of five in predicted and measured values. However, the agreement is surprisingly good considering the fact that, especially in the joint region, the tibia deviates considerably from an ideal cylindrical tube and reliable predictions of strains induced in the joint region are not possible with such simple models.

Adequate stimulation of the slit sense organs. Electrophysiological experiments (ref. Barth 1981) have proven that the slit sense organs respond selectively to slit compression. Loads which lead to compression of the organs were predicted from a simple mechanical model (framework) of the tibia-metatarsus joint. In general these predictions have been verified by direct measurements at the actual tibia. This is especially true for the dependence of compression on the tibia-metatarsus angle, α, during axial load. The different shapes of the strain-force characteristics during anterior and posterior deflection are probably due to a change of the effective levers at the tibia-metatarsus joint, in other words to a lateral shift of the centre of rotation. The higher sensitivity of most organs to hemolymph pressure is perhaps caused by direct expansion of the cuticle, which compounds the strain induced by joint load.

Furthermore, these strain measurements are supported by photoelastic investigations, using Araldite models (Barth and Pickelmann 1975). In these experiments too, loading of the tibia-metatarsus joint by muscle forces results in a compression of the organs at the lateral tibia and in a dilatation of the organ VS5 at the ventral tibia.

3.4 Comparison with electrophysiological data

Since the present measurements are the first strain measurements on arthropods, similar studies are not available for a further comparison with electrophysiological data. Measurements exist for the organ HS8 under lateral load (theraphosid, see Fig. 24; *Cupiennius* $\alpha = 130°$: Barth and Bohnen-

berger 1978; Bohnenberger 1981), and investigations on the elicitation of reflexes (*Cupiennius*) by the organs HS8, HS9 and VS4 under lateral load ($\alpha = 130°$) and dorso-ventral load (limit, $\alpha = 200°$, Seyfarth 1978a). In agreement with the strain measurements, it has been proven that the organ HS8 ($\alpha = 130°$) is stimulated by posterior deflection and the organ VS4 by anterior deflection.

The lyriform structure of the organs opens up a broad linear working range (Barth and Bohnenberger 1978; Bohnenberger 1981): Shorter slits (fast adapting) respond to greater forces and thus higher strains and longer slits (slow adapting) respond to smaller forces. Thus, under axial or lateral load, a straightened leg does not simply lead to a lower response, but shifts the strain signal into a region where especially the longer slits are sensitive. In contrast, flexion of the leg shifts the strain signal into the linear range of shorter slits.

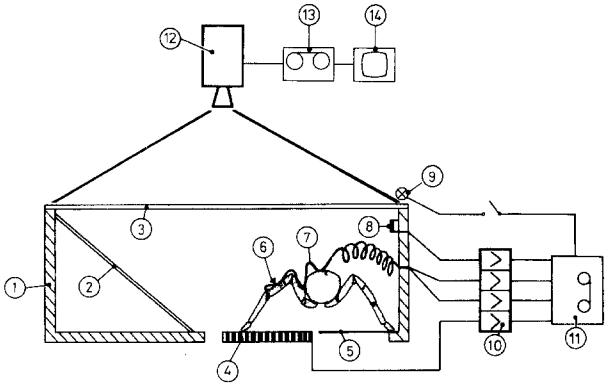

Fig. 25. Apparatus for simultaneous measurement of leg kinematics, strains in the cuticle, ground reaction force and hemolymph presure. *1* track; *2* mirror; *3* cover of 'plexiglas'; *4* force plate; *5* ground membrane; *6* pressure transducer; *7* wires; *8* temperature sensor; *9* light emitting diode; *10* amplifier and filter; *11* fm-tape recorder; *12* video camera; *13* video recorder; *14* monitor

3.5 Calculation of strains occurring in freely moving animals

In freely walking animals, strains at the site of the organs can be calculated by multiplying the axial, lateral, and dorsoventral component of the instantaneous ground reaction force with the corresponding mechanical sensitivities, and summing the resultant strain values (principle of linear superposition; example in Chapter IV). At the tibia-metatarsus joint this procedure is facilitated by a special joint structure. Hemolymph pressure and muscle force are antagonistic at this joint, and they control only the dorsoventral component of the ground reaction force. If the hemolymph pressure is also measured, even strains developed by the internal parameters can be assessed.

IV. Strains in freely moving animals

In this part of the study we applied miniature strain gauges to the cuticle at the various sites of lyriform organs near the tibia-metatarsus joint of theraphosids. We attempted to measure the magnitude of strains developed here, and to see how they differ during slow locomotion. By comparing it with the load pattern, we were able to study the specialization of the various organs to perceive specific load.

1 Material and methods

Apparatus. The video system used to record the spiders' locomotion allowed for a time resolution of 50 frames/s (Fig. 25; recorder: NV-8030, National; camera: Video Guard 720 C, Jai). In the 50 cm long image sector we chose, the errors of the co-ordinates relative to the animal's center were less than 2%. The errors introduced by transferring measurements from the TV-image onto tracing paper amounted to less than 1 mm. The video- and fm-tape could be synchronized precisely with the signal of a light emitting diode.

Signals provided by the strain gauges applied to the animal, by the pressure transducer, and by the force plate were amplified (factor: 63,000), filtered ($f_0 = 80$ Hz Bessel 24 dB/oct; own development), and stored on fm-tape together with the LED-signal. All data was digitized (MOP AMO2 Digiplan, Kontron) and stored with a computer (Minc 11, Digital).

Data evaluation: The following points were considered:

a) To facilitate the comparison of the different time courses of movements and strains, all readings were standardised in the following way: The time for one step was taken as 100% and the steep rise in the vertical leg excursion (z_1), at the onset of a return stroke, was chosen as a marker of the beginning of the step (Fig. 26).

b) The momentary tibia-metatarsus angle α had to be determined as it greatly affects the amount of strain (see Chapter II).

c) A transformation of the force components from global to local co-ordinates (Goldstein 1963) was necessary to allow an interpretation of the strain values measured during locomotion on the basis of strains induced in tethered animals. The global co-ordinates are oriented parallel to the edges of the track. The local ones are (i) parallel to the metatarsus (z'), (ii) perpendicular to the main plane of the movement of the tibia-metatarsus joint (y') and (iii) in the main plane of movement (x').

d) Negative strain in the surrounding cuticle induces compression of the slit sense organs. The assessment of strain sign necessitates a definition of the *zero level*. The zero level chosen here is the resting value, measured prior to and just after walking. This is the same procedure as is commonly used in vertebrate studies (cf. Lanyon et al. 1975; Carter et al. 1980).

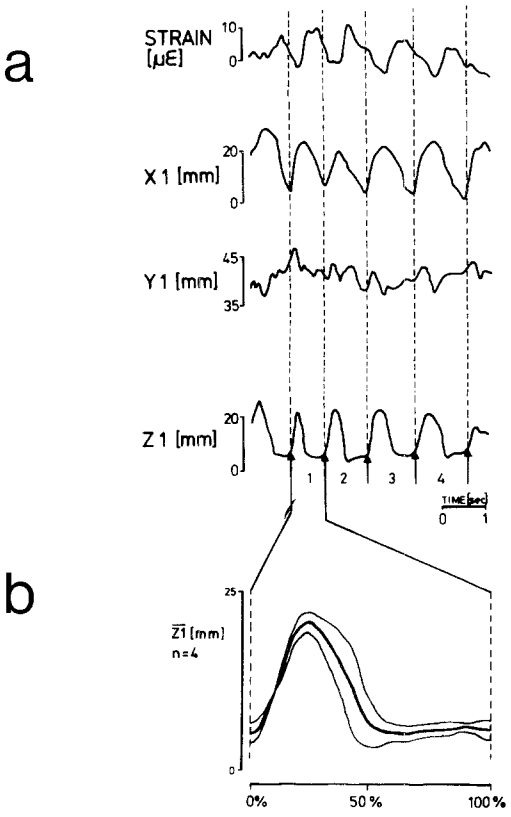

Fig. 26a, b. Description of leg kinematics and strain time relationship. (Animal: Samantha; walk number: L18; 2nd leg; site of strain measurement: compound slit sense organ HS8 – parallel to the slits). **a** Time course of the co-ordinates of the tibia-metatarsus joint (x_1: longitudinal, y_1: lateral, z_1: vertical) and the simultaneously measured strain. —— beginning of promotion; *1, 2, 3, 4* steps. **b** Averaging and standardization of the vertical component of the leg excursion (z_1; ±SD)

2 Results

2.1 Leg kinematics

Strains measured in the leg skeleton depend on load, which is correlated with kinematics. A detailed observation of leg kinematics is necesary to decide whether the time courses of the strains measured are typical for the specific sites of measurement, or can be attributed to differences in the leg movement. To guarantee compatible experimental conditions, slow (1 to 10 cm/s) and smooth walking movements were selected.

Step length, periods of motion and animal velocity: the animal's velocity v and the step frequency f are related as follows:

$$v = 5.7 \cdot f^{1.5} \text{ cm/s.} \quad (10)$$

From this equation, the step length ($l = v/f$) can be derived:

$$l = 5.7 \cdot f^{0.5} \text{ cm.} \quad (11)$$

Relative to the whole step, the length of the power stroke is almost independent of the walking speed (48% ±2 SD).

Kinematics of the second leg. The normalized time relationship of the metatarsus-tip excursion relative to the body (cf. Fig. 26) varies even during the same walking bout (Fig. 29). Interindividual variation is of the same order of magnitude.

The time course of the *vertical* component (z_1) of the leg movement has an almost triangular shape during the return stroke; up- and downstrokes are executed at about the same rates. The vertical excursion increases with running speed from ca. 10 mm (2 cm/s) to 20 mm (10 cm/s).

The *horizontal* component of motion (x_1) shows the same triangular shape, but with a faster stroke forwards and a plateau indicating a cautious placing of the leg. The mean value of the excursion is 20 mm ±0.3 SD.

The *lateral component,* perpendicular to the animal's long axis (y_1) remains almost constant (38 mm ±2 SD) during locomotion.

Similarly, the *joint angle* α between the tibia and the metatarsus, calculated from the co-ordinates of the patella-tibia, the tibia-metatarsus, and the metatarsus-tarsus joint, shows little variation ($\alpha = 178° \pm 4$ SD; mean standard deviation in different walks: 13° ±6 SD).

Differences among legs. The time courses of the leg excursions are similar for the second leg in different animals, but the same parameters vary widely in different legs (Fig. 31). This is clearly seen when plotted in a cyclic graph (Fig. 27).

The *vertical* excursion (z_1) increases from the fourth to the first leg. The *horizontal* excursion (x_1), which determines the step length, is similar for the second to fourth legs. It is, however, distinctly shorter for the first leg. Correspondingly, the first leg is pulled towards the body during the return stroke, and such *lateral* excursion (y_1) is small for all other legs. The value of the *joint angle* varies within the same small range of 160° to 180° in all legs (Fig. 31). In the second to fourth legs, the maximum excursion *velocities* of the leg tip relative to the body occur at the beginning of the return stroke. The velocity is decreased with the start of each power stroke.

2.2 Strain and leg excursion

2.2.1 Strains in the second leg

Strain amplitudes. Preliminary experiments had demonstrated that blinded tarantulas, during slow

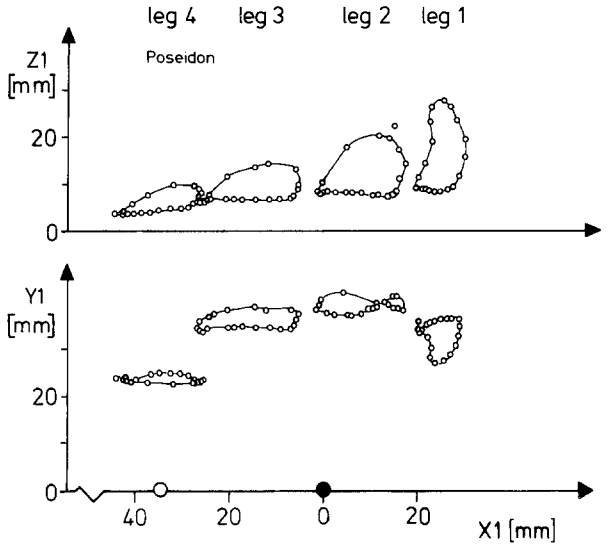

Fig. 27. Excursion of the metatarsus-tarsus joint (cyclic diagram). Above: lateral view (x, z); below: dorsal view (x, y); • centre of prosoma; o centre of opisthosoma

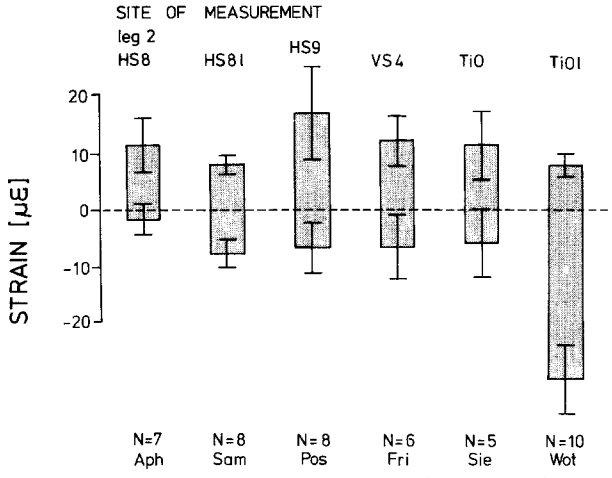

Fig. 28. Average strain amplitude (±SD) during slow locomotion (2nd leg) at the site of the slit sense organs *HS8, HS9, VS4, VS5* (*l*: parallel to the slits, otherwise at right angle) and at the dorsal tibia (*TiO* at the right angle to long tibial axis, *l* parallel to it). *N* number of walks, each walk consists of 3 to 6 steps; 'zero'-strain: value measured at the resting animal

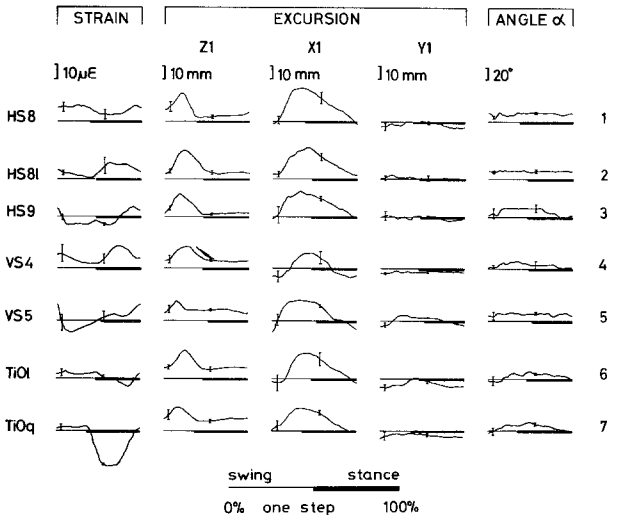

Fig. 29. From left to right: time courses (*i*) of the strains at the site of different slit sense organs at the distal tibia, (*ii*) of the leg excursion in vertical (z_1), longitudinal (x_1), and lateral (y_1) direction, and (*iii*) of the tibia-metatarsus joint angle (±SD; 2nd leg; one step: 100%). The time courses of the leg excursions are very similar (exception: 5, limping animal), whereas the time courses of strains differ. Ordinate values marked by the level calibration bars and of the x-axes: *strain:* 0 με (resting value); z_1: 0 mm; x_1: 0 mm, y_1: 40 mm (origin is the vertical projection of the prosoma center onto the track floor); tibia-metatarsus angle: 160°. (*1* to *7* represent different animals; *1*: Aphrodite L24; *2*: Samantha L18; *3*: Poseidon L32; *4*: Friedrich L37; *5* Boris L3; *6*: Siebenbeinige L18; *7*: Wotan L9)

locomotion, used the first leg frequently like a feeler. Consequently, arrhythmic, irregular load changes were expected. In contrast, the second leg is loaded rhythmically, and the expected change during each step from lateral to dorsoventral load facilitates the study of the role of the various slit sense organs, which are particularly sensitive to lateral loads.

Strain amplitudes (pp, see Fig. 28), measured across the lyriform organs, *HS8, HS9* and *VS4* (i.e., at right angle to the long axes of the slits), are similar (19 με ± 5 SD). In all cases, the positive values are significantly larger than the negative ones ($P<0.01$; differences in the individual positive values: $P>0.01$ and in the negative values: *HS8* and *HS9* $P<0.001$, otherwise, $P>0.05$). The strain differences, measured in parallel and at a right angle to the slits long axes (*l, q*) of lyriform organ *HS8*, are similar (16 με and 13 με, respectively; $P>0.05$).

In contrast, strains measured on the same side of the dorsal tibia, above a muscle attachment, are considerably smaller (17 με) in a direction perpendicular to the long tibial axis than they are when parallel to it (38 με). The negative values for the parallel direction are the largest measured in the tibia of the second leg ($P<0.001$).

Time courses. Strains vary periodically with every step at all measurement sites. The strain maxima and minima, measured at a right angle to the long axes of the different slit sense organs, occur at different times during a particular step (Fig. 29).

Site of organ *HS8:* Perpendicular to the slits' long axes, the strain decreases early in the power

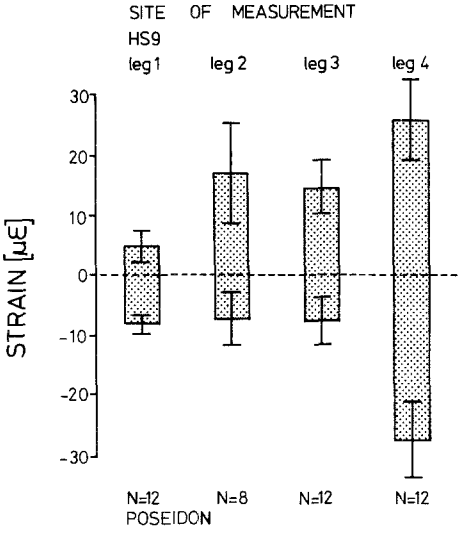

Fig. 30. Strain amplitudes (±SD) at different legs of the same animal at the site of the organ *HS9*. Leg *1, 2, 3* measured simultaneously; leg *2* different walk

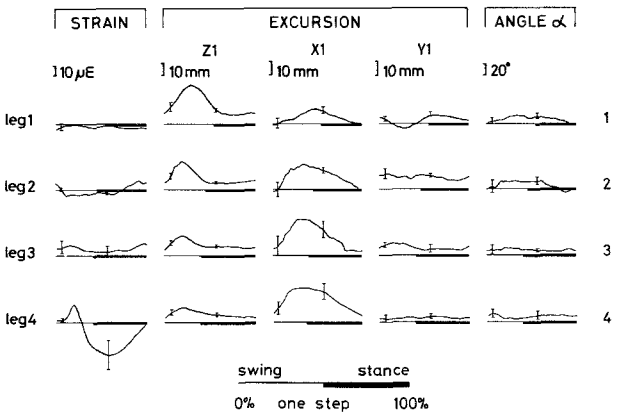

Fig. 31. Time courses of (*i*) the strain (*HS9*, Poseidon) measured at different legs of the same animal, (*ii*) of the leg excursions, and (*iii*) of the tibia-metatarsus angles (±SD). Strain time relationships are very similar especially for the 3rd and 4th leg. Strain drops before the beginning of the stance with lowering of the leg. The fourth leg is hardly lifted, the onset time of the stance is not marked clearly. Strain measured at the first leg is low. For all legs the tibia-metatarsus angle is similar (from 160° to 180°). Ordinate values are given by calibration bars and by the level of the x-axes (only given if different from Fig. 29): y_1: 30 mm; x_1: 20 mm (*1*), 0 mm (*2*), −30 mm (*3*), −60 mm (*4*) (*1* to *4* different walks; *1*: L11; *2*: L32; *3*: L11; *4*: L11)

stroke, when the leg is put down. At the end of the power stroke, strain increases to the same value that it reaches during the return stroke. Parallel to the slits' long axes, the strain-time relationship is almost inverted with respect to the zero-level.

Site of organ *HS9:* Here, the strain already decreases during the beginning of the return stroke. During the power stroke it rises to a strain value similar to that at the site of the organ HS8.

Site of organ *VS4:* Strains measured at this organ are lowest during the return stroke, but they do not drop below the resting value and they reach a maximum during the power stroke.

Site of organ *VS5:* A marked strain minimum occurs during the return stroke and values are largest during the power stroke.

Site of dorsolateral *muscle attachments* on tibia: During the power stroke, the strain drops when measured in a direction perpendicular and parallel to the long axis of the tibia.

2.2.2 Strains developed in the cuticle of different legs

Strain amplitudes. Strains were measured simultaneously in legs 1, 3, and 4. The strain amplitudes at *HS9* increase from the first to the fourth leg (Fig. 30). This is especially true for the positive part ($P<0.001$), whereas the negative strain values are significantly larger only in the fourth leg ($P<0.001$).

Time courses. Considering differences in leg excursions, one would predict for the first leg a time course of the strains which is different from that of the others. In accordance with its weak and arrhythmic load, strain remains almost constant and very low (Fig. 31), whereas in the other legs the strain readings display high rhythmical variations. The time courses measured in the third and fourth leg are similar: strains rise as the legs are lifted and drop as they are lowered; they reach a minimum early in the power stroke and after its mid-portion they rise to the initial value.

The measurements on the second leg, done in separate experiments, already display a strain drop during the early return stroke and the strain rises during the power stroke, as in the third and fourth leg. In no leg is the onset of the power stroke marked by a distinct change in the strain value.

2.3 Strains during fast locomotion

The maximum animal velocity recorded was 56 cm/s (Aphrodite L6). The kinematics of the legs change with velocity. In the second leg, with increasing velocity, the horizontal forward excursion of the leg tip with respect to its coxa diminishes and the leg is clearly stretched backwards during the power stroke. The maximum strain measured was 120 με (organ VS4, Friedrich L22). In all cases, the strain value rises with the walking speed. A quick start produces a fast rise in strain, which

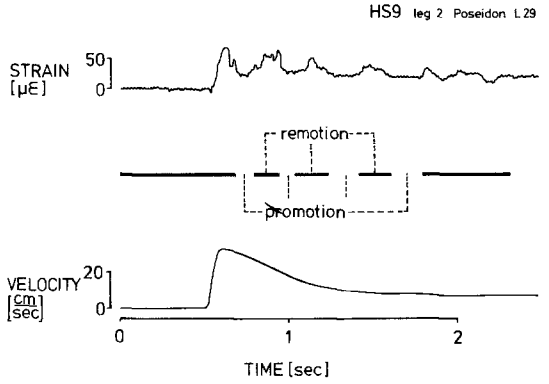

Fig. 32. Strain at the site of the organ *HS9*, step pattern, and velocity of the animal

declines again with a decrease in running speed (Fig. 32). The strains vary synchronously with the step cycle; however, the strain maximum, which occurred during the end of the power stroke or the beginning of the return stroke in slow locomotion, is now shifted towards the middle of the power stroke.

2.4 Spectral strain density

Using spectral analysis, one can test which strain frequencies predominate in the experiments performed (Fig. 33). According to electrophysiological experiments the receptor response of slit sensilla is more easily elicited by high rather than low frequency stimuli (Barth and Bohnenberger 1978; Bohnenberger 1981). From this information, it seems safe to conclude that the strain value monitored by the organ is also frequency dependent, i.e., the response to fast changes of strain is more pronounced.

The spectrum[1], obtained during slow locomotion (Fig. 33a) displays a maximum at the step frequency (0.53 Hz$\pm$0.03 SD, $n=8$). On average (Fig. 33b), the power envelope above 0.5 Hz decreases in proportion to f^{-2}. From this, the spectral density of the strain amplitude *sd* can be deduced. Above 0.6 Hz the envelope satisfies the equation:

$$sd = 36.5 f^{-1}\ \mu\varepsilon\ \text{s}. \qquad (12)$$

For a walk including faster movements, high frequencies become more prominent. In the representative walk shown in Fig. 33c, the shift of the ener-

[1] Spectrum: Spectral density of the deformation energy $e=E$ strain$^2/4\,F_0$; Young's modulus $E=18$ GPa; sample time $1/F_0=9.76$ s. A spectrum obtained at the resting animal and therefore containing the noise of the apparatus was subtracted

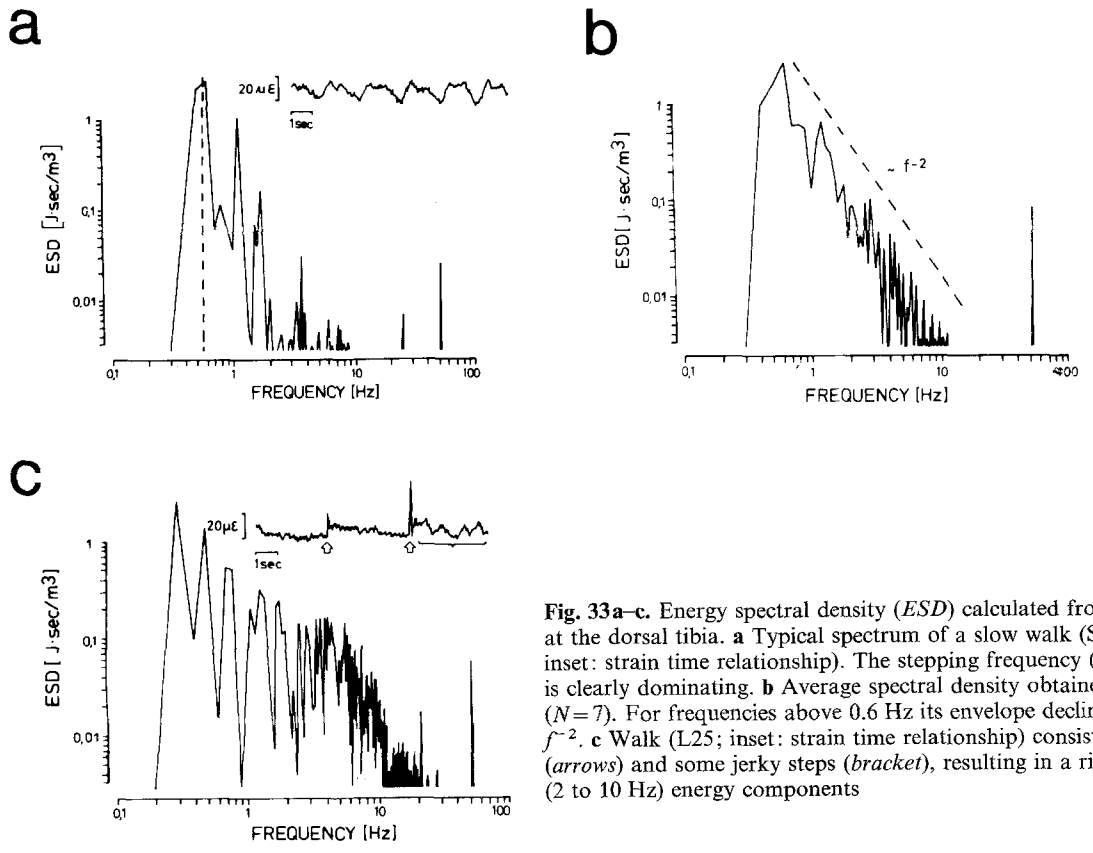

Fig. 33a–c. Energy spectral density (*ESD*) calculated from strains measured at the dorsal tibia. **a** Typical spectrum of a slow walk (Siebenbeinige L23; inset: strain time relationship). The stepping frequency (0.53 Hz$\pm$0.03 SD) is clearly dominating. **b** Average spectral density obtained during slow walk ($N=7$). For frequencies above 0.6 Hz its envelope declines proportional to f^{-2}. **c** Walk (L25; inset: strain time relationship) consisting of some jumps (*arrows*) and some jerky steps (*bracket*), resulting in a rise of highfrequent (2 to 10 Hz) energy components

gy between 2 Hz to 20 Hz is due to jumping of the spider.

2.5 Simultaneous measurement of kinematics, strain, ground reaction force, and hemolymph pressure

The amplitude and time course of the skeletal strains are determined by the internal and external forces developed during locomotion, but can not be deduced from kinematics. The relevant *external* force during slow locomotion is the ground reaction force; *internal* forces include the muscle forces acting at a particular joint and the hemolymph pressure. If both the external force and the hemolymph pressure are known, the moment developed by muscles can be determined. Taking this and the measured ground reaction force, the expected strains can be calculated and compared with the observed ones.

In one animal the strain at the site of the lyriform organ HS8 (fourth leg) was measured during slow locomotion together with the hemolymph pressure in the dorsal blood channel (see Chapter II), the ground reaction force, and the tibia-metatarsus angle ($n=6$; Fig. 34). The latter remained constant at approximately $175° \pm 10$ SD. The observed strain drop coincided with the rise in the ground reaction force. By contrast the hemolymph pressure remained almost constant at about 2.6–3.3 kPa. One can thus conclude that the strain drop measured is caused by muscle forces compensating for the ground reaction force.

2.6 Actual measurement versus linear superposition of component strains

According to the principle of linear superposition, strains developed by natural loads at the lyriform organs can be calculated by adding the strains induced by the different load components.

In the fourth leg, the hemolymph pressure rises at the start of the walk from 2.2 kPa ± 1 SD to 5.3 kPa. No external forces act during the return stroke (the leg mass is small), so the moments developed by hemolymph pressure and muscles are equal with opposite signs. This results in strains of the same magnitude but with opposite signs (sum equal to 0 με; see Chapter III).

In a standing spider the load is half that in a walking animal, because the weight is distributed over eight instead of four legs. A muscle force of ca. 7 mN is necessary to compensate for the moment produced by a hemolymph pressure of 5.3 kP (for calculation see Chapter II).

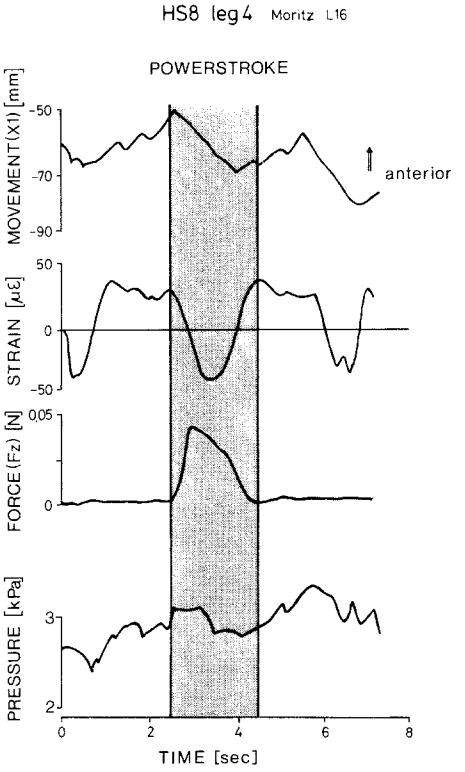

Fig. 34. From above to below, simultaneous measurement of (*i*) horizontal *deflection* of the 2nd leg, (*ii*) *strain* at the site of the organ *HS8*, (*iii*) vertical component of the ground reaction *force*, and (*iv*) the *hemolymph pressure* in the tibia. During the stance the strain drops by about −80 με. Hemolymph pressure remains low and almost constant

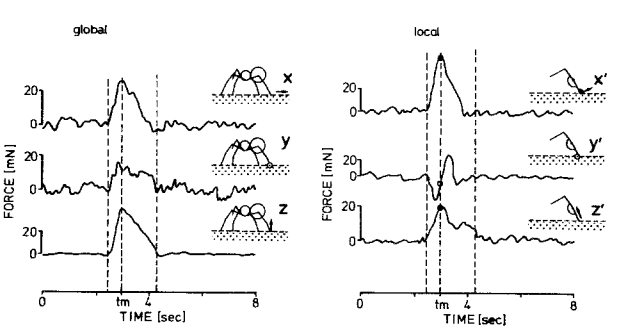

Fig. 35. Components of the ground reaction force (see Fig. 34 and Table 2) in global co-ordinates (parallel to the track) and local co-ordinates (parallel to the metatarsus; attend to different scales; t_m: time of maximum vertical force)

A transformation of the co-ordinates, from the global system in which the ground reaction force has been measured to the local one, allows to determine the dorsoventral (*Fx'*), lateral (*Fy'*), and axial (*Fz'*) force components (Fig. 35). Considering a dorso-ventral force component of 40 mN, a maximum muscle force of 200 mN is possible. The pressure rise elicited by this force can be expected to

Table 2. Force components measured at t_m (see Fig. 35), mechanical sensitivity measured for the organ HS8 (strain/force; see Chapter III) and strains obtained by multiplication of force and sensitivity. The dorso-ventral force component (Fx′) induces the strain drop measured at the free walking animal

Moritz/Kroton HS8	Force (max) [n]	Strain/ force [με/N] $\alpha=175°$	⇒	Strain [με]
Fx′ (dorso-ventral)	0.04	−2,500	⇒	−100
Fy′ (anterior-posterior)	0	0	⇒	0
Fz′ (proximal-distal)	0.02	100	⇒	2

be 0.4–0.5 kPa. In Table 2, the values of the force components at the time of maximum load (t_m), the corresponding mechanical sensitivities of the organ ($\alpha=175°$), and the resulting strain (product of sensitivity and force) are listed. The sum of these strains ($S=-98$ με), which is the maximum value expected during the power stroke, is in good agreement with the actual measurement of -80 με.

2.7 Slit sense organs as strain detectors

Stimulus amplitude. During slow locomotion (2nd leg) the strain values perpendicular to the slits' long axes reach about 20 με at the sites of all tibial lyriform organs. Taking the special geometry of organ HS8 into account, the largest compression of the most compliant slit is less than 3 nm. During slow locomotion no organ receives particularly high inputs; the main difference is in their time course.

Measurement of load during slow locomotion – Temporal pattern of strains. Using our measurements, the following picture may be drawn of the strain measurement by slit sense organs in the spider's tibia:

HS8: As explained previously, no compression or dilatation can be expected during the return stroke. During the power stroke, however, the organ is stimulated. Active propulsion (developed in proximal joints) leads to a dilatation and therefore reduces stimulation. During slow locomotion, the organ senses the moments, developed by muscles, during the power stroke.

For all other organs, statements about stimulating conditions are more complex.

HS9: Since this organ is more sensitive to extension than to flexion of the metatarsus, one would expect its dilatation during the return stroke. However, with a sufficiently high ground reaction force and during active propulsion this organ may be stimulated during the power stroke.

VS4: Arguments about the stimulation of this organ are similar to those given for organ HS9; the mechanical sensitivities during extension and flexion are similar for both. A dilatation during the return stroke can therefore also be expected for the organ VS4. During a strong propulsion of the spider, and in contrast to HS9, a dilatation of the slits occurs during the power stroke as well, such that the organ is not compressed at any time during undisturbed locomotion.

VS5: This organ is the only one compressed by a rise in hemolymph pressure. It can be stimulated during the return stroke of the stepping cycle due to a higher sensitivity to extensions of the metatarsus.

TiO: A single slit parallel to the tibial long axis can measure the activity of the Fl.met.bil.. For a slit oriented at a right angle to the long tibial axis, it is not possible to clearly correlate adequate stimulation with muscle-force or hemolymph pressure (see Chapter III).

Stimulation of organs in different legs. In spite of differences in the positions of the various legs, organs HS8 and HS9 are stimulated during about the same phase of the stepping cycle in the second and fourth legs. However, the differences in position lead to a rise in the strain amplitudes from the second to the fourth leg.

3 Discussion

3.1 Leg kinematics

Stepping frequency. In spite of very different conditions stepping frequency, running speed, and step period obtained for unrestrained animals walking on a track are consistent with previous measurements during faster, compensated locomotion (Kramer-sphere; Seyfarth and Bohnenberger 1980).

Leg kinematics. Leg movements are mainly determined by leg rotation in the coxa-trochanter joint (dorsal-ventral, anterior-posterior) and the femur-patella joint (dorso-ventral). Although joint mechanics allows for a change of more than 90° in the tibia-metatarsus angle (Blickhan, in prep.) only a change of 20° was measured during slow locomo-

tion. A larger rotation at the tibia-metatarsus joint occurs only during fast locomotion. An increase, with running speed, in the angle of limb rotation as found in the spider is also known for bipedal and quadrupedal locomotion of vertebrates (Charteris et al. 1979). The flexion of a leg during the return stroke reduces its moment of inertia. During slow locomotion, forces of inertia play only a minor role and flexion at the tibia-metatarsus joint is not necessary, as long as the proximal joint produces the movement.

Special role of first leg. Relative to the other legs, the power stroke of the first leg is shorter and its vertical excursion is higher. Together with the low strain values, this indicates that during slow locomotion this leg has an additional feeler function as suggested for the first leg of the stick insect (Cruse 1976).

3.2 Loads, developed by internal and external forces

According to findings in the stick insect (multiple point bearing arch; Cruse 1976) and the cricket (Harris and Chiradella 1980), a ground reaction force parallel to the metatarsus was expected. Such a load condition would reduce the mechanical moments developed at distal joints and remove load from peripheral muscles, which, under these circumstances, only have to stabilize the joints. Furthermore, propulsive forces of the hind legs have to overcome the repulsive forces developed by the forelegs.

If the force vector were indeed directed parallel to the metatarsus, one would predict on the basis of the mechanical sensitivity of the organ HS8 that there would be zero strain during power stroke. By contrast, the strain and force measurements presented in this paper indicate that the ground reaction force is not directed parallel to the metatarsus and flexion predominates extension at the tibia-metatarsus joint.

3.3 Strains

Equally distributed strength of the spider's tibia. The strain values measured in the cuticular exoskeleton of spiders ($<120\ \mu\varepsilon$) are small compared to the peak values reached in the leg bones of vertebrates (e.g. sheep, horses, humans: $<850\ \mu\varepsilon$; Lanyon et al. 1975; the Young's Modulus for bone is similar to that for spider cuticle; see Chapter I). The similarity of the strain amplitudes measured at different sites of the spider tibia suggests that, by way of proper shaping, material distribution and degree of sclerotisation, the mean strain occurring in the tibia during natural load is kept constant; in other words, the tibia has an equally distributed strength.

Strain rates. The highest strain rates measured in the exoskeleton of spiders (ca. 1 $\mu\varepsilon$/ms) are much below the values measured in the leg bones of vertebrates (ca. 13 $\mu\varepsilon$/ms). In spiders, particularly during slow locomotion, the spectral density of the strain is inversely proportional to the frequency, above 0.5 Hz (Eq. 12). Since strains are proportional to applied load (see Chapter III) one would expect a similar spectral density of the ground reaction force.

3.4 Strain reception and locomotion

Thresholds. The force threshold above which a response of the organ HS8 was measured during lateral deflection (8 mN, see Chapter III) is considerably lower than the forces, measured during slow locomotion (40 mN). The strains (50 $\mu\varepsilon$) developed by this lateral load at the site of the organ HS8 are within the same range as those measured during locomotion, i.e. the organ would be stimulated.

The highpass characteristics of the receptor emphasizes the higher frequencies (Bohnenberger 1981), but does not result in a shift of the maximum of the receptor response from the leg's step frequency during slow locomotion. However, during fast locomotion and jumps this filtering leads to a shift of the maximum receptor response to higher frequencies, even if the absolute maximum of the spectral strain amplitude remains at lower frequencies.

Reflexes. Electrophysiological investigations have shown that load dependent reflexes contribute to the control of locomotion in cats and cockroaches. The end of the power stroke is linked with release of the load onto the leg. Similar reflexes exist for spiders (*Cupiennius,* Seyfarth 1978a). Relatively large (with respect to threshold stimulation of the lyriform organs) lateral deflections are necessary to elicit these reflexes through stimulation of the lyriform organs located around the tibia-metatarsus joint. Especially at the site of organ HS8, the strains induced by lateral and axial load increase with leg flexure (Chapter III), and the reflex may be brought about by a lower load in a flexed leg. For flexion of the leg increases with running speed, such a reflex may be more easily elicited at high animal velocities.

All of our results suggest the stimulation of

the lyriform organs HS8, HS9, and VS4 by the activity of the flexor muscles. Under dorsoventral loads, a reflex not influenced by slit sense organs was found only at the dorsal limit of limb rotation (resistance reflex; Seyfarth 1978a, b). Under this load condition, only a stimulation of the organ VS5 can be deduced from strain measurements. In between the dorsal and ventral limits of limb rotation, a strong stimulation of the organs is only possible in passive deflection (see Chapter III) at high deflection rates, or if the activity of the flexor muscles is high.

Strain receptors in the tibia of the cockroach (campaniform sensilla) also elicit reflexes during locomotion (Zill and Moran 1981a, b; Zill et al. 1981). Two different receptor groups trigger extensor muscle activity during the power stroke, and flexor muscles during the end of the power stroke, respectively. In both cases, muscle activity reduces the excitation of these receptors, which suggests a negative feedback loop. If one postulates a similar mode of receptor operation at the tibia-metatarsus joint of spiders, a compression of the organ HS8 would induce a rise in the hemolymph pressure. During slow locomotion, however, the pressure in the tibia remains almost constant.

Role of slit sense organs. So far, there have been only few clear clues as to the role of load sensitive organs in arthropod locomotion control. A mechanical insight into the stimulation mechanisms of such receptors in behavioural situations is still in its early stages. In general, strain receptors seem to elicit reflexes, which serve to decrease skeletal load. Measurements with tethered animals indicate that there are load conditions which elicit only small strains at an organ in spite of high loads. Reducing strain in the organ's region by changing the leg's position with respect to the ground reaction force, therefore, does not result in a reduction of load at the tibia metatarsus joint. Considering stability of the leg's and the animal's position, a regulation simply leading to a minimum load cannot be expected. However, our measurements suggest a regulation leading to a less dangerous situation for the leg skeleton by changing the legs' position with respect to external load and by a reduction of load peaks.

Acknowledgements. Thanks are due to Dr. H. Bleckmann, Mr. A. Brüssel, Miss K. Longworth and Mr. J.W. Ruthven for critically reading the manuscript. The authors gratefully acknowledge the help received from Mrs. M. Dresken, Mr. U. Scheuring, Mrs. S. Fischer and Mrs. B. Janouscheck. Supported by a grant of the Deutsche Forschungsgemeinschaft to F.G. Barth (SFB 45/A2).

References

Adam M, Czihak G (1964) Mikroskop und mikroskopische Arbeitsmethoden. Fischer, Stuttgart

Alexander RMcN (1979) The invertebrates. University Press, Cambridge

Allan W, Charlton M, Montgomery A (1980) Semiconductor force transducer suitable for use with small muscles. Med Biol Eng Comput 18:378–380

Arcan M (1982) Experimental stress analysis and biomechanics: Their current interaction. Proc VII Intern Conf Exp Stress Analysis, Haifa:61–79

Baggot DG, Goodship AE, Lanyon LE (1981) A quantitative assessment of compression plate fixation in vivo: An experimental study using the sheep radius. J Biomech 14:701–711

Barnes GRG, Pinder DN (1974) In vivo tension and bone strain measurement and correlation. J Biomech 7:35–42

Barth FG (1973) Microfiber reinforcement of an arthropod cuticle. – Laminated composite materials in biology. Z Zellforsch 144:409–433

Barth FG (1978) Slit sense organs: 'Strain gauges' in the arachnid exoskeleton. Symp Zool Soc Lond 42:439–448

Barth FG (1981) Strain detection in the arthropod exoskeleton. In: Laverack MS, Cosens DJ (eds) Sense organs. Blackie, Glasgow, pp 112–141

Barth FG, Blickhan R (1984) Mechanoreception. In: Bereiter-Hahn J, Matoltsy AG, Richards KS (eds) Biology of the integument, vol 1. Springer, Berlin Heidelberg New York Tokyo, pp 554–582

Barth FG, Bohnenberger J (1978) Lyriform slit sense organ: thresholds and stimulus amplitude ranges in a multi unit mechanoreceptor. J Comp Physiol 125:37–43

Barth FG, Libera W (1970) Ein Atlas der Spaltsinnesorgane von *Cupiennius salei* Keys. (Chelicerata Araneae). Z Morphol Tiere 68:343–369

Barth FG, Pickelmann P (1975) Lyriform slit sense organs: modelling an arthropod mechanoreceptor. J Comp Physiol 103:39–54

Barth FG, Seyfarth E-A (1979) *Cupiennius salei* Keys. (Araneae) in the highlands of central Guatemala. J Arachnol 7:255–263

Barth FG, Ficker E, Federle HU (1984) Model studies on the mechanical significance of grouping in compound spider slit sensilla (Chelicerata, Araneida). Zoomorphology 104:204–215

Bayer R (1968) Untersuchungen am Kreislaufsystem der Wanderheuschrecke (*Locusta migratoria migratorioides* R. et F., Orthopteroidea) mit besonderer Berücksichtigung des Blutdruckes. Z Vergl Physiol 58:76–135

Blickhan R, Barth FG (1979) Dehnungen und Spannungen im Außenskelett von Arthropoden. In: VDI, Experimentelle Spannungsanalyse in der Werkstofftechnik. GESA-Symp., Braunschweig, S

Blickhan R, Barth FG, Ficker E (1982) Biomechanics in a sensory system. (Strain detection in the exoskeleton of arthropods.) Proc VII'th Int Conf Exp Stress Anal, Haifa, 223–234

Bohnenberger J (1978) The transfer characteristics of a lyriform slit sense organ. Symp Zool Soc Lond 42:449–455

Bohnenberger J (1979) Das Übertragungsverhalten eines zusammengesetzten Spaltsinnesorganes auf dem Spinnenbein. Dissertation, Frankfurt am Main

Bohnenberger J (1981) Matched transfer characteristics of single units in a compound slit sense organ. J Comp Physiol 142:391–402

Burger JW, Smythe CHMcC (1953) The general form of circulation in the lobster, *Homarus*. J Cell Comp Physiol 42:369–383

Carter DR (1978) Anisotropic analysis of strain rosette information from cortical bone. J Biomech 11:199–202
Carter DR, Smith DJ, Spengler DM, Daly CH, Frankel VH (1980) Measurement and analysis of in vivo bone strains on the canine radius and ulna. J Biomech 13:27–38
Chapman G (1958) The hydrostatic skeleton of invertebrates. Biol Rev 33:338
Chapman G (1975) Versatility of hydraulic systems. J Exp Zool 194:24
Charm SE, Kurland GS (1972) Blood rheology. In: Bergel DH (ed) Cardiovascular fluid dynamics. Academic Press, London, pp 158–195
Charteris J, Leach D, Taves C (1979) Comparative kinematic analysis of bipedal and quadrupedal locomotion: a cyclographic technique. J Anat 128:803–819
Cochran GVB (1972) Implantation of strain gauges on bone in vivo. J Biomech 5:119–123
Cortrell CB (1962) The imaginal ecdysis of blowflies. Observations on the hydrostatic mechanisms involved in digging and expansion. J Exp Biol 39:431–448
Cruse H (1976) The function of the legs in the free walking stick insect, *Carausius morosus*. J Comp Physiol 112:235–262
Currey JD (1967) The failure of exoskeletons and endoskeletons. J Morphol 123:1–16
Darnhofer-Demar B (1977) Funktionsmorphologie der Mittelbeine von Wasserläufern der Gattung *Gerris*. Fortschr Zool 24:115–122
Elliott CJH (1981) The expansion of *Schistocerca gregaria* at the imaginal ecdysis: The mechanical properties of the cuticle and the internal pressure. J Insect Physiol 27:695–704
Galilei G (1638) Untersuchungen und mathematische Demonstrationen über zwei neue Wissenszweige, die Mechanik und die Fallgesetze betreffend. Arectri. Ostwalds Klassiker 11, 24, 25. Wiss Buchges, Darmstadt (1973)
Glücklich D (1976) Die Versteifung von Kunststoffmodellen durch elektrische Dehnungsmeßstreifen. VDI-Zeitschrift 118:829–834
Goldstein H (1963) Klassische Mechanik. Akad Verlagsges, Frankfurt
Harris JK (1978) A photoelastic substrate technique for dynamic measurements of forces exerted by moving organisms. J Microscopy 114:219–228
Harris J, Ghiradella H (1980) the forces exerted on the substrate by walking and stationary crickets. J Exp Biol 85:263–279
Heglund (1981) A simple design for a force plate to measure ground reaction forces. J Exp Biol 93:333–338
Hepburn HR, Joffe I (1976) On the material properties of insect exoskeletons. In: Hepburn HR (ed) The insect integument. Elsevier, Amsterdam, pp 207–235
Hergenröder R, Barth FG (1983) The release of attack and escape behavior by vibratory stimuli in a wandering spider (*Cupiennius salei* Keys.). J Comp Physiol 152:361–371
Lanyon LE (1972) In vivo bone strain recorded from thoracic vertebrae of sheep. J Biomech 5:277–281
Lanyon LE, Hampson WGJ, Goodship AE, Shah JS (1975) Bone deformation in vivo from strain gauges attached to the human tibial shaft. Acta Orthop Scand 46:256–268
Lanyon LE, Smith RN (1969) Measurements of bone strain in the walking animal. Res Vet Sci 10:93–94
Lauder GV, Lanyon LE (1980) Functional anatomy of feeding in the bluegill sunfish, *Lepomis macrochirus:* In vivo measurement of bone strain. J Exp Biol 84:33–55
Melchers M (1963) Zur Biologie und zum Verhalten von *Cupiennius salei* (Keyserling), einer amerikanischen Ctenide. Zool Jb Abt System, Oekol Geogr 91:1–90
Müller RK (1971) Handbuch der Modellstatik. Springer, Berlin Heidelberg New York
Nachtigall W (1977) Biostatik. In: Hoppe W, Lohmann W, Markl H, Ziegler H (eds) Biophysik. Springer, Berlin Heidelberg New York, pp 514–525
Parry DA (1957) Spider leg-muscles and the autotomy mechanism. Q J Microsc Sci 98:331–340
Parry DA, Brown RHJ (1959a) The hydraulic mechanism of the spider leg. J Exp Biol 36:423–433
Parry DA, Brown RHJ (1959b) The jumping mechanism of salticid spiders. J Exp Biol 36:654–664
Pauwels F (1949/50) Die Bedeutung der Bauprinzipien des Stütz- und Bewegungsapparates für die Beanspruchung der Röhrenknochen. Z Anat Entwickl Gesch 114:129–167
Picken LER (1936) The mechanism of urine formation in invertebrates. I. The excretion mechanism in certain Arthropoda. J Exp Biol 13:309–328
Roberts VL (1966) Strain-gauge techniques in biomechanics. Exp Mech 6:19–23
Seyfarth E-A (1978a) Lyriform slit sense organs and muscle reflexes in the spider leg. J Comp Physiol 125:45–57
Seyfarth E-A (1978b) Mechanoreceptors and proprioceptive reflexes: lyriform organs in the spider leg. Symp Zool Soc Lond 42:457–467
Seyfarth E-A, Barth FG (1972) Compound slit sense organs on the spider leg: Mechanoreceptors involved in kinesthetic orientation. J Comp Physiol 78:176–191
Seyfarth E-A, Bohnenberger J (1980) Compensated walking of tarantula spiders and the effect of lyriform slit sense organ ablation. Proc 8. Int Congr Arachnol, Wien, pp 249–255
Slama K (1976) Insect hemolymph pressure and its determination. Acta Entomol Bohemoslov 73:65–75
Stewart DM, Martin AW (1974) Blood pressure in the tarantula, *Dugesiella hentzi*. J Comp Physiol 88:141–172
Speck J, Barth FG (1982) Vibration sensitivity of pretarsal slit sensilla in the spider leg. J Comp Physiol 148:187–194
Szabo I (1972) Höhere technische Mechanik. Springer, Berlin Heidelberg New York
Szabo I (1975) Einführung in die technische Mechanik. Springer, Berlin Heidelberg New York
Tanaka Y, Hisada M (1980) The hydraulic mechanism of the predatory strike in dragonfly larvae. J Exp Biol 88:1–19
Vincent JF, Hillerton JE (1979) the tanning of insect cuticle – A critical review and a revised mechanism. J Insect Physiol 25:653–658
Wainwright SA (1969) Design in hydraulic organisms. Naturwissenschaften 57:321–326
Wright TM, Hayes MC (1979) Strain gauge application on compact bone. J Biomech 12:471–475
Yamada H (1970) Strength of biological materials. Evans FG (ed) Williams and Willkins, Baltimore
Zdarek J, Slama K, Gottfried F (1979) Changes in internal pressure during puparium formation in flies. J Exp Zool 207:187–196
Zill SN, Moran DT (1981a) The exoskeleton and insect proprioception. I. Responses of tibial campaniform sensilla to external and muscle-generated forces in the American cockroach, *Periplaneta americana*. J Exp Biol 91:1–24
Zill SN, Moran DT (1981b) The exoskeleton and insect proprioception. III. Activity of tibial campaniform sensilla during walking in the American cockroach, *Periplaneta americana*. J Exp Biol 94:57–75
Zill SN, Moran DT, Varela FG (1981) The exoskeleton and insect proprioception. II. Reflex effects of tibial campaniform sensilla in the American cockroach, *Periplaneta americana*. J Exp Biol 94:43–55